

Insights into the northward shift of Pacific cod in warming Bering Sea waters from pop-up satellite archival tags

Julie K. Nielsen ^a, Susanne F. McDermott^b, Kimberly M. Rand ^c, Elizabeth J. Dawson ^b, David Bryan ^b, Lyle Britt^b, Stan Kotwicki ^b, and Daniel G. Nichol^b

^aKingfisher Marine Research, LLC, 1102 Wee Burn Dr., Juneau, AK 99801, USA; ^bNational Oceanic and Atmospheric Administration, National Marine Fisheries Service, Alaska Fisheries Science Center, 7600 Sand Point Way Northeast, Seattle, WA 98115, USA; ^cLynker (Under Contract to National Oceanic and Atmospheric Administration, National Marine Fisheries Service, Alaska Fisheries Science Center), 202 Church Street SE #536, Leesburg, VA 20175, USA

Corresponding author: Julie K. Nielsen (email: julie.nielsen@gmail.com)

Abstract

The summertime distribution of Pacific cod in the Bering Sea shifted dramatically northward into the Northern Bering Sea (NBS) during 2017–2019 in conjunction with unprecedented ocean warming. In 2019, we tagged 38 NBS Pacific cod with pop-up satellite archival tags during summer foraging to characterize seasonal migration to winter spawning locations. Geolocation results for 31 Pacific cod indicate that tagged Pacific cod moved out of the NBS shelf area beginning in November ahead of oncoming winter sea ice. Most tagged fish (77% geolocation probability) moved to traditional spawning areas in the Eastern Bering Sea during the peak spawning period, but some crossed international and internal management boundaries by moving into Russian waters and the Gulf of Alaska (16% and 7% geolocation probability, respectively). Our results demonstrate that Pacific cod are tightly coupled to seasonal environmental changes and suggest that recent northward shifts in summertime distributions are tied to warm-water expansion of foraging habitat. Our findings underscore the need for adaptive management strategies to address the challenges of shifting fish distributions under changing environmental conditions.

Key words: demersal fish, geolocation, seasonal migration, electronic tagging

Introduction

Poleward shifts in distribution have been observed for many fish species in response to a changing climate (Perry et al. 2005). The magnitude and orientation of climate-related distributional shifts can vary by species, depth range, and region (Campana et al. 2020). Fish may move poleward to maintain optimal physiological conditions such as temperature and oxygen levels or to exploit newly available habitats and food resources; range shifts can occur through larval dispersal or movement of adults (Pinsky et al. 2020). Understanding the mechanisms that underlie distributional shifts in response to changing environmental conditions is important for predicting the effects of a changing climate for individuals, populations, and communities (Pinsky et al. 2020) as well as adopting proactive management strategies (Bell et al. 2020).

Northward distribution shifts have recently been observed for the Bering Sea region of the North Pacific Ocean (Stafford et al. 2022), which spans 54 to 66 degrees latitude and is bordered by Alaska to the east and Russian waters to the west. The Bering Sea is an extremely productive subarctic region that is dominated by annual winter sea ice coverage over a

relatively shallow (30–150 m) shelf. Seasonal sea ice produces a summertime cold pool with bottom temperatures between –2 and 2 °C that has historically limited the northward distribution of sub-Arctic fish. Gradual northward shifts in sub-Arctic fish distributions have been observed in conjunction with declining sea ice and subsequent northward contraction of the cold pool (Mueter and Litzow 2008). However, a period of intense warming occurred in the Bering Sea from 2017 to 2019 that led to severely decreased or even non-existent annual cold pool extent (Siddon 2021). During this period, the summertime distributions of many marine species from the Eastern Bering Sea (EBS) shifted substantially northward into the Northern Bering Sea (NBS) and even into the Arctic (Stevenson and Lauth 2019; Stafford et al. 2022; Levine et al. 2023).

Pacific cod (*Gadus macrocephalus*) is one of the species that experienced a dramatic northward shift in its summertime Bering Sea distribution during the abnormally warm years of 2017–2019 as determined by survey catch data (Stevenson and Lauth 2019). Pacific cod is a commercially and ecologically important demersal gadid that is widely distributed across the North Pacific Ocean and is known to undertake

large-scale movements between summer foraging and winter spawning areas (Shimada and Kimura 1994; Rand et al. 2014; Bryan et al. 2021). The Bering Sea Pacific cod stock is assessed based on an annual Alaska Fisheries Science Center (AFSC) groundfish and crab bottom trawl survey (Markowitz et al. 2024) which surveys the EBS every year and is extended into the NBS in some years. The majority of the Pacific cod biomass in the Bering Sea has historically been located in the EBS (Stevenson and Lauth 2019). However, in the abnormally warm years of 2017–2019, the NBS proportion of the Bering Sea Pacific cod population increased substantially (Thompson and Thorson 2019). Pacific cod biomass in the AFSC NBS survey increased 887% between 2010, a colder year, and 2017 and continued to increase in 2019 (Markowitz et al. 2022).

This rapid northward shift of Pacific cod into the NBS, where few cod were observed prior to 2017 (Stevenson and Lauth 2019), prompted a number of questions related to the management of the Bering Sea stock. What was the spatial and temporal nature of the northward shift? Was it a short-term expansion of summer foraging areas during warm summers followed by return to traditional spawning areas in the EBS in the winter? If so, what environmental conditions were associated with movement to or from the NBS? Or was it a permanent shift to the NBS, where fish remained year-round and potentially spawned? Were more fish moving into Russian waters as the distribution shifted north? Answers to these questions were needed to understand the best way to incorporate the northward distribution shifts into stock assessment (Thompson and Thorson 2019), ensure that the current management practice of treating NBS and EBS as the same population was correct (Barbeaux et al. 2023), and to develop proactive adaptive approaches to management of Pacific cod in changing environmental conditions (Bahri et al. 2021).

To address these questions, in 2019 we initiated a pop-up satellite tagging program to provide detailed information on the seasonal and annual movement patterns of Pacific cod in the NBS. Pop-up satellite tags (PSATs) measure and record depth, temperature, and light data. PSATs are programmed to release from the fish on a specified date and transmit their data to the Argos satellite network, thus providing a wealth of fishery-independent data about the movement and behavior of the fish during the tag deployment period. The location of the tag when it first pops up and the transmitted data can be used to reconstruct movement pathways to estimate a daily location along with associated daily location error (Nielsen and Sibert 2007; Pedersen et al. 2008). Depth and temperature data from the PSATs provide important information about habitat occupied and relationships with environmental conditions. Thus, PSATs offer a number of advantages over conventional tags. Conventional tags require large numbers of tags to be released over multiple years, rely on recapture in the commercial fishery, and only provide information on release and recovery locations. Additionally, PSATs can track movement outside of fisheries surveys which can only be conducted in the summer months, are limited in spatial extent, and do not provide information about individual fish movement trajectories.

The goals of the PSAT study were to use pop-up locations and reconstructed movement paths to understand the sea-

sonal movement patterns of Pacific cod tagged in the NBS. Specifically, we sought to (1) characterize areas occupied during the peak spawning period (February 15–March 31), (2) determine if and when cod left the NBS during seasonal migrations and whether seasonal movement was related to environmental conditions such as temperature and sea ice extent, and (3) determine whether tagged fish returned to the NBS the following summer. We discuss our results in terms of implications for understanding seasonal movement of Pacific cod in the Bering Sea, seasonal movement between management areas, and implications for adaptive management in a changing climate.

Materials and methods

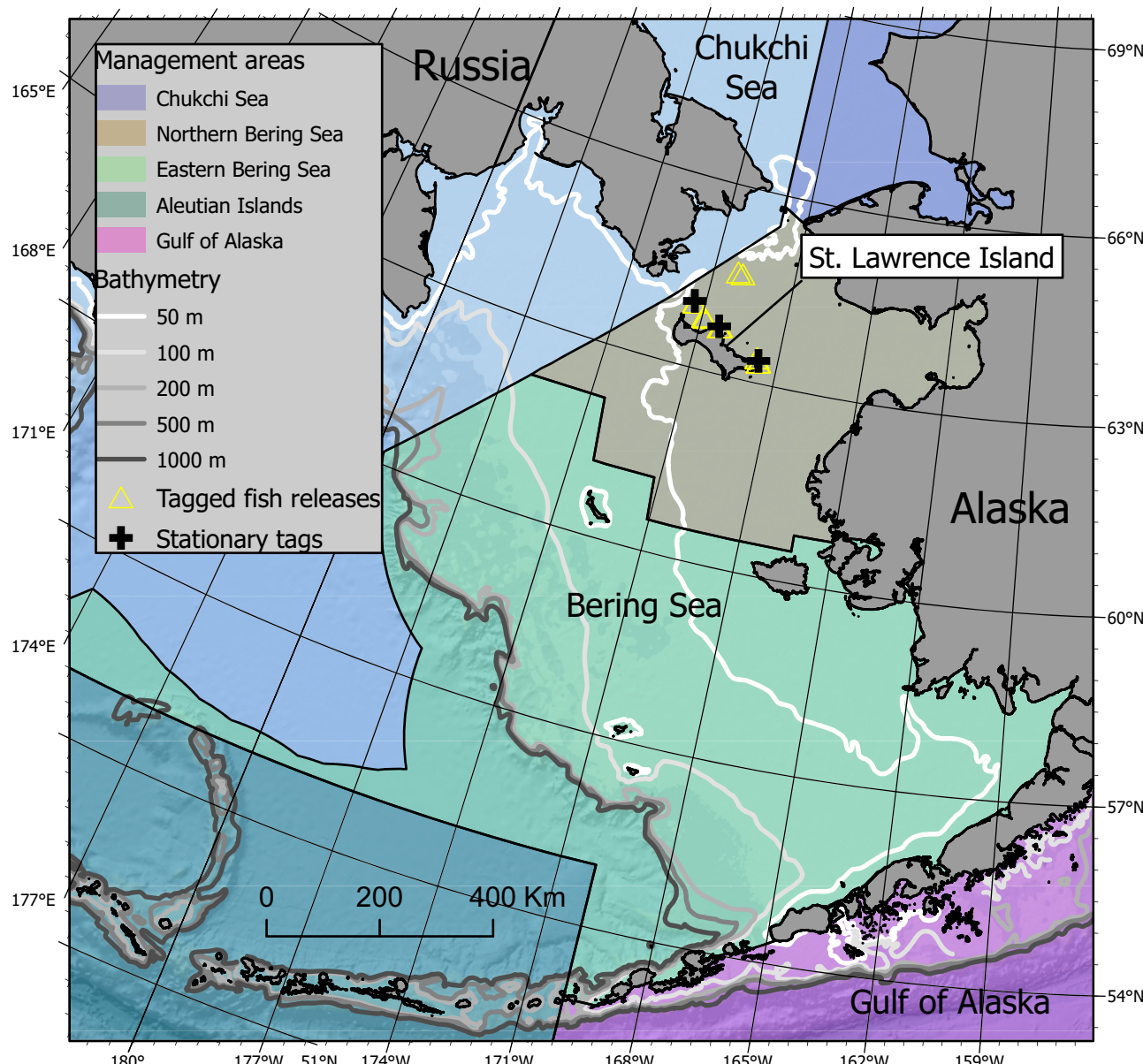
Capture and tagging

During August–September 2019, adult Pacific cod were tagged with Pop-up Satellite Archival Tags (PSATs, also referred to as “satellite tags”) from two release platforms in the NBS: the annual National Marine Fisheries Service (NMFS) summer bottom-trawl survey (“survey”; Markowitz et al. 2022) and the Native Village of Savoonga (Fig. 1). On the survey, fish were captured by rod and reel from survey vessels FV Alaska Knight and FV Vesteraalen. In Savoonga, fish were captured by handline from the FV Scarlett and the FV Adeline. We followed accepted standards and ensured the ethical treatment of captured fish, including guidelines from the U.S. Government Principles for the Utilization and Care of Vertebrate Animals Used in Testing, Research, and Training (<https://olaw.nih.gov/policies-laws/gov-principles.htm>) and the American Fisheries Society Guidelines for the Use of Fishes in Research (https://fisheries.org/docs/policy_useoffishes.pdf; Chapter V). Research was conducted under NOAA Scientific Research Permit 2019–5.

Satellite tags were attached to adult Pacific cod using a harness with spectra line, following Bryan et al. (2021). Tagging methods were adjusted slightly from Bryan et al. in the following ways to improve tagging outcomes: (1) fish were tagged immediately after capture without being placed in a holding tank to minimize surface time and barotrauma effects; (2) we used smaller diameter hypodermic needles in the custom jig; and (3) the harnesses were attached between the first and second dorsal fin instead of anterior of the first dorsal fin. Immediately after tagging, fish were released with a descender at a depth of 15 or 30 m, depending on water depth. In Savoonga only, captured fish that did not receive a PSAT were tagged with two bright orange, individually numbered Floy T-bar tags (referred to as “conventional tags”). Conventional tags were inserted into the musculature on the right and left upper dorsal area beneath the first fin using a Floy tag insertion gun for a total of two tags per fish. Conventional tags were recovered in commercial fisheries where recoveries were reported to NMFS biological observers aboard fishing vessels or at fish processing plants. Additional details about capture and tagging are available in Markowitz et al. (2025).

The satellite tags deployed in this study were MiniPAT tags manufactured by Wildlife Computers, Inc. (Redmond, WA).

Fig. 1. Bering Sea study area. Management regions for Pacific cod in Alaska are indicated by colored polygons. Fish tagging locations in the Northern Bering Sea are indicated by yellow triangles. Stationary satellite tags (black crosses) were deployed in areas where tagged fish were released. Base map: ArcGIS World Ocean Base (ESRI 2011). Map projection: Albers Equal Area Conic, UTM. Map datum: NAD 1983.



The MiniPAT satellite tags were 124 mm long, 38 mm wide, and weighed 60 g in air. They recorded information on depth (0–1700 m, resolution 0.5 m), temperature (−40–60 °C, resolution 0.05 °C), tri-axial acceleration (−2 to 2 g, resolution 0.05 g), and light levels ($5 \times 10^{-12} \text{ W.cm}^{-2}$ – $5 \times 10^{-2} \text{ W.cm}^{-2}$) at intervals ranging from 1 to 5 s depending on programmed deployment duration. To allow transmission of recorded data to the satellite network, which is limited by tag battery life, data were summarized to provide: (1) light levels during dawn and dusk, from which longitude was estimated using GPE2 software from Wildlife Computers; (2) daily minimum and maximum temperature and depth; and (3) temperature-depth profiles in 12 h time bins. Because

the performance of the PSATs (e.g., transmission rates, geolocation) for this study area was initially uncertain, tags were programmed to release from the fish at a variety of time intervals (90, 150, 180, 210, 300, or 360 days) to obtain known locations throughout the year. Time-series data for different deployment durations were generated at different time intervals to limit the amount of data transmitted: 300 s for 90-day tags, 450 s for 150- and 180-day tags, 600 s for 210-, 300-, and 360-day tags. For 300- and 360-day tags, depth and temperature time series were both generated on alternate days. If a tag was physically recovered, the entire archived high-resolution dataset was available for analysis.

Stationary tags were deployed near release sites to assist geolocation by providing information about light-based longitude precision and a record of bottom temperatures over the course of the study. Three stationary MiniPAT satellite tags were deployed for a 12-month period near three tag release locations in the NBS (Fig. 1). Stationary tag moorings consisted of a 30 kg anchor with a 1 m section of floating polymer rope and a 20 cm hard plastic T-float (Bryan et al. 2021). Depth time series (600 s intervals) were recorded every other day. Light intensity during dusk and dawn and temperature time series data (600 s intervals) were recorded every day. Longitude estimates were obtained using Wildlife Computers GPE2 software. The root mean square error (RMSE) between light-based longitude estimates and known stationary tag longitudes was calculated and used to select the variance used to derive light-based longitude likelihoods for the geolocation model (see below).

Analyses

Geolocation

A hidden Markov model (HMM) originally developed for the geolocation of Atlantic cod in the North Atlantic (Pedersen et al. 2008) and adapted for the geolocation of Pacific cod in the Aleutian Islands (Nielsen et al. 2023b) was used to estimate daily locations of satellite-tagged Pacific cod in the Bering Sea. Full model description and details are available in Nielsen et al. (2023b). Briefly, the model is a discrete state-space model that operates on a grid of the study area and consists of coupled movement and data likelihood models. The movement model is isotropic diffusion, with different movement states (e.g., foraging vs. migrating) possible through the use of different values of diffusion for each state. The data likelihood model provides information on the likelihood of observing light-based longitude and maximum daily depth from the tagged fish for each study area grid cell on each day. The model consists of a forward-filter, where probability from the previous day is updated first by the movement model and then the data likelihood model, followed by backward smoothing to incorporate information from the end location. The resulting model output provides the probability that the tagged fish occupied each study area grid cell on each day.

The study area was divided into 3 km² grid cells (575 × 589 cells). For the maximum depth likelihood, bathymetry data for the study area was obtained from the Alaska Region Digital Elevation Model (ARDEM, <http://research.cfos.uaaf.edu/bathy/>, Danielson et al. 2015) and aggregated to obtain the mean and standard deviation of depth for each model grid cell. The likelihood value for depth for each grid cell was calculated by integrating a normal probability curve of the mean grid cell depth and standard deviation between the maximum daily depth measured by the tag plus and minus tag measurement uncertainty (Le Bris et al. 2013). For the light-based longitude likelihood, longitude estimates were obtained from Wildlife Computers GPE2 software (Wildlife Computers 2012) and manually filtered to exclude observations more than 2 degrees from the previous day. The likelihood value for light-

based longitude consists of the probability of observing the longitude estimated from tag data given a normal distribution with a mean of grid cell longitude and a standard deviation derived empirically from stationary tag data. We used a value of 1.5 degrees for the standard deviation, a value slightly larger than observations obtained from stationary tag data (this study and Nielsen et al. 2023b). Likelihoods for depth and longitude were combined using cell-wise multiplication. Longitude and depth gradients are roughly orthogonal in the Bering Sea (Fig. 1). Therefore, the intersection of these gradients provides location information without the use of light-based latitude, which is much less precise and reliable than light-based longitude.

Through the use of movement states, it is possible to incorporate smaller values of diffusion for a fish when it is likely not moving much (e.g., foraging) and a larger value of diffusion when the fish is likely moving more (e.g., migration). Because the geolocation gradients during migration were strong in our study, we preferred to keep the model simple and estimate one value of diffusion for the entire trajectory. Diffusion is estimated by maximum likelihood using the forward filter alone (Thygesen et al. 2009), then the most likely value of diffusion is used in the forward filter with backward smoothing to obtain daily probabilities for each grid cell. For some sparse data sets we used two movement states. Trajectories were divided into summer foraging and winter migrating movement states based on the mean migration initiation date estimated by net squared displacement (NSD) analyses (see below). To obtain a diffusion rate for summer foraging, we averaged the maximum likelihood diffusion estimates from all fish with pop-up dates that were earlier than the estimated migration initiation date. To obtain a diffusion rate for winter migrating, we averaged maximum likelihood diffusion estimates from all fish with pop-up dates later than the estimated migration initiation date.

Pathways were reconstructed for each fish for which archival data from the PSAT was available. Point locations were estimated for each day using the Viterbi algorithm (Nielsen et al. 2023b), that provides the most probable sequence of grid cells occupied each day based on the posterior probability. Points estimated from the Viterbi algorithm are the center of most probable grid cell for each day. Estimated error in geolocation estimates was determined by generating polygons that encompassed the highest 50% and 99% of the posterior probability on each day.

For each geolocated fish, posterior probabilities were summarized by month and during the peak of the spawning period (February 15 to March 31). Location probabilities were summarized and normalized by day to account for differing number of days per month available for each fish. Composite probability surfaces for all tagged animals were generated by cell-wise averaging of summarized probabilities for all fish. The proportion of overall probability in the NBS, EBS, Russian waters, and Gulf of Alaska (GOA) regions was calculated for monthly and peak spawning period probability surfaces. Sea ice extent data was obtained in vector format from the National Snow and Ice Data Center (U.S. National Ice Center 2010) and added to composite probability plots.

Migration timing and extent

NSD analyses can be used to identify directed movement that occurs when animals migrate between breeding and foraging areas and also to quantify migration timing and extent (Bunnefeld et al. 2011; Börger and Fryxell 2012). We applied NSD analyses to the estimated daily Viterbi point locations derived from the geolocation model to estimate winter spawning migration timing and extent for the population of tagged fish with pop-up dates of January 2020 or later. Detailed information about NSD analyses is provided in Supplementary Data S1. Briefly, we used the NSD statistic (the squared net distance between the tagging location and the model-estimated daily fish location at each time step) to identify the individual data sets that fit a migration NSD pattern (i.e., directed movement to a spawning location). The migration NSD pattern is represented by a logistical curve with parameters of an asymptote, which represents migration spatial extent, as well as midpoint and scale that together represent migration timing. Migration timing and extent were then estimated for the “population” of tagged fish found to have the migration NSD pattern using a nonlinear mixed-effects model (package “nlme,” Pinheiro et al. 2021) in R. Date was converted to number of days since 1 August 2019 to provide a time scale that would accommodate annual movement from summer to summer. Data sets for fish at liberty through the summer of 2020 were truncated to 13 March 2020 to match maximum deployment lengths of winter 2020 pop-up tags. Tag ID was treated as a random effect; the most parsimonious random effects structure (e.g., which fixed effects were allowed to vary by Tag ID) was determined by assessing the individual variation among parameter estimates from individual (nls) fits and likelihood ratio tests for mixed-effects models that converged (Pinheiro and Bates 2000). First degree autocorrelation was estimated as a term in the model, as the Viterbi locations output by the HMM are highly autocorrelated.

PSAT depth and temperature data

We assessed monthly patterns in maximum daily depth as well as daily minimum and maximum temperatures to understand environmental conditions experienced during summer foraging, winter migration, and spawning periods. Maximum daily depth is assumed to approximate the seafloor depth for demersal fishes (Nichol et al. 2007; Nielsen et al. 2019), and thus is an additional method to geolocation for visualizing seasonal movement from the shallow (60 m 90% quantile depth) NBS. Daily minimum and maximum temperatures provide information on thermal conditions tolerated by Pacific cod in different seasons.

Barotrauma recovery time was assessed by manual inspection of depth records to exclude observations obtained during the recovery period from depth analyses. Barotrauma recovery was identified as a pattern of initial movement between deep water during the day and shallow water at night, with gradually increasing minimum depths each day until daily depth change did not differ markedly from the rest of the trajectory (Nichol and Chilton 2006; Bryan et al. 2021).

To account for different data densities from satellite-transmitted compared to physically recovered tags, we based analyses on daily values and used mixed-effects models to account for different data set resolution among tags. Each environmental value (daily maximum depth, daily maximum temperature, and daily minimum temperature) was fit to a mixed-effects model with month (August 2019 to June 2020) as a fixed-effect variable and Tag ID as a random effect variable using restricted maximum likelihood. We also compared monthly models to null (random intercept only for Tag ID) and a season fixed-effect (April–November = summer, December–March = winter) with a random Tag ID effect and maximum likelihood estimation. Residual analysis and diagnostics were conducted to ensure linear mixed-effects model assumptions were met (Zuur et al. 2009).

All modeling and analysis was performed using R version 4.3.2 (R Core Team 2023).

Results

Capture and tagging

PSATs were deployed on 38 Pacific cod; 30 fish were released during the survey and 8 were released from the Native Village of Savoonga (Fig. 1, Table 1). The average size of fish released from the survey was 68 cm (range: 56–78 cm); the average size of fish released from Savoonga was 70 cm (range: 52–90 cm) (Table 1). The average duration of barotrauma recovery was 4 days and ranged from 2 to 6 days (Table 1). Depth at release locations averaged 27 m (s.d. 5.8 m). Additional details about capture and tagging results are available in Markowitz et al. (2025).

Conventional tags ($n = 86$) were only released from the Native Village of Savoonga. The average size of conventional tagged Pacific cod was 67 cm (range: 52–90 cm). Six conventional tags were returned by the commercial fishery and used as additional information on known fish locations at time of recapture (Table 2).

Three stationary satellite tags were deployed at depths of 31, 32, and 36 m (Fig. 1). Two of the three stationary tags (tag 183939, Savoonga, and tag 183940, western St. Lawrence) successfully transmitted data from deployment durations of 362 and 328 days, respectively. The third stationary tag did not transmit at all.

Satellite tag data

Pop-up locations were obtained for 33 of 38 PSAT-tagged fish (Table 1, Fig. 2). We did not observe any PSAT tag-related mortality, defined as non-fishery mortality that occurs within the first four weeks after tagging. The average number of Argos messages received (excluding fisheries recaptures) was 1834 (s.d. 1178).

Of the 33 PSATs that reported to satellites, 18 (55%) reported on the scheduled date of pop-up. Seven PSAT-tagged fish (21%) were recaptured by commercial fishing vessels. One PSAT-tagged fish (Tag 183961) was captured by a vessel in Russian waters, but the tag was not physically recovered. Therefore, a total of six PSATs were physically recovered and provided detailed (1 s to 5 s) data sets. Seven

Table 1. Satellite tag releases and recoveries from two platforms during the summer in 2019: National Marine Fisheries Service (NMFS) bottom trawl survey (August) and Native Village of Savoonga (September).

| Tag ID | Rel date | Rel lat | Rel long | Depth (m) | Length (cm) | Rec date | Rec lat | Rec long | Rec region | Barotr (days) | Days at liberty |
|---------|-----------|---------|----------|-----------|-------------|------------|---------|----------|------------|---------------|-----------------|
| 183942 | 8/14/2019 | 63.41 | -168.76 | 25 | 61 | 11/13/2019 | 61.70 | -167.70 | NBS | 4 | 90 |
| 183943 | 8/14/2019 | 63.35 | -168.68 | 25 | 70 | 11/13/2019 | 60.57 | -171.27 | EBS | 4 | 90 |
| 183945 | 8/14/2019 | 63.35 | -168.68 | 25 | 64 | 1/25/2020 | 57.23 | -170.69 | EBS | 4 | 184 |
| 183947* | 8/14/2019 | 63.35 | -168.68 | 25 | 77 | 2/20/2020 | 57.20 | -171.07 | EBS | 3 | 190 |
| 183948 | 8/14/2019 | 63.35 | -168.68 | 25 | 73 | 6/13/2020 | 62.51 | -173.65 | NBS | 4 | 300 |
| 183949* | 8/14/2019 | 63.35 | -168.68 | 25 | 73 | 10/23/2019 | 64.67 | -167.93 | NBS | 3 | 70 |
| 183950 | 8/14/2019 | 63.35 | -168.67 | 25 | 71 | 3/19/2020 | 54.33 | -161.94 | WGOA | 4 | 218 |
| 183951 | 8/14/2019 | 63.35 | -168.68 | 25 | 67 | 2/28/2020 | 58.22 | -173.48 | EBS | 4 | 189 |
| 183952 | 8/11/2019 | 64.03 | -171.40 | 29 | 71 | 11/10/2019 | 62.21 | -169.17 | NBS | 4 | 90 |
| 183953 | 8/11/2019 | 64.03 | -171.40 | 29 | 61 | 11/10/2019 | 63.64 | -172.37 | NBS | 5 | 90 |
| 183954 | 8/11/2019 | 64.03 | -171.40 | 29 | 64 | 11/10/2019 | 63.73 | -171.41 | NBS | 5 | 90 |
| 183955 | 8/10/2019 | 63.85 | -170.95 | 23 | 76 | 11/10/2019 | 63.70 | -171.19 | NBS | 5 | 91 |
| 183956 | 8/9/2019 | 64.65 | -169.95 | 46 | 66 | 1/10/2020 | 63.27 | -175.52 | RUS | 4 | 151 |
| 183957 | 8/11/2019 | 64.03 | -171.40 | 29 | 62 | 1/9/2020 | 60.42 | -172.05 | EBS | 4 | 151 |
| 183958 | 8/11/2019 | 64.03 | -171.40 | 29 | 68 | 3/12/2020 | 62.16 | -177.59 | RUS | 5 | 211 |
| 183959 | 8/10/2019 | 63.84 | -170.90 | 23 | 74 | 3/10/2020 | 60.75 | -178.42 | EBS | 4 | 212 |
| 183960 | 8/9/2019 | 64.67 | -170.13 | 48 | 67 | 3/8/2020 | 59.25 | -175.16 | EBS | 4 | 211 |
| 183961† | 8/11/2019 | 64.03 | -171.40 | 29 | 76 | 11/8/2019 | 63.13 | -176.88 | RUS | 4 | 85 |
| 183962* | 8/11/2019 | 64.03 | -171.40 | 29 | 78 | 10/26/2019 | 64.84 | -167.67 | NBS | 3 | 76 |
| 183963 | 8/11/2019 | 64.03 | -171.40 | 29 | 74 | 12/23/2019 | 65.20 | -168.62 | NBS | NA | 134 |
| 183964 | 8/11/2019 | 64.03 | -171.40 | 29 | 67 | 2/7/2020 | 63.17 | -176.55 | RUS | 4 | 153 |
| 183965 | 8/11/2019 | 64.03 | -171.40 | 29 | 70 | 6/7/2020 | 58.21 | -158.73 | EBS | 4 | 300 |
| 183968* | 8/10/2019 | 63.85 | -170.96 | 23 | 68 | 9/3/2019 | 64.04 | -170.38 | NBS | 3 | 24 |
| 183970 | 8/11/2019 | 64.03 | -171.40 | 29 | 63 | 1/21/2020 | 59.98 | -171.40 | EBS | 6 | 162 |
| 183971* | 8/11/2019 | 64.03 | -171.40 | 29 | 71 | 3/22/2020 | 59.99 | -175.75 | EBS | 4 | 223 |
| 184057 | 9/9/2019 | 63.75 | -170.27 | 42 | 61 | 12/9/2019 | 64.05 | -172.65 | RUS | 4 | 90 |
| 184058 | 9/8/2019 | 63.75 | -170.31 | 42 | 64 | 12/9/2019 | 63.44 | -173.98 | RUS | 4 | 91 |
| 184059 | 9/8/2019 | 63.75 | -170.32 | 42 | 83 | 3/8/2020 | 57.95 | -173.83 | EBS | 5 | 181 |
| 184060‡ | 9/9/2019 | 63.75 | -170.28 | 42 | 68 | 6/1/2020 | 63.89 | -171.84 | NBS | 4 | 112 |
| 184061 | 9/8/2019 | 63.75 | -170.32 | 42 | 70 | 3/8/2020 | 59.43 | -175.88 | EBS | 5 | 181 |
| 184062 | 9/8/2019 | 63.75 | -170.32 | 42 | 66 | 9/6/2020 | 63.74 | -170.32 | NBS | NA | 361 |
| 184063 | 9/8/2019 | 63.75 | -170.32 | 42 | 71 | 7/8/2020 | 61.51 | -168.33 | NBS | NA | 304 |
| 184064* | 9/8/2019 | 63.75 | -170.32 | 44 | 73 | 9/12/2019 | 63.99 | -169.77 | NBS | 2 | 4 |

Note: The latitude and longitude for release and recovery are shown in decimal degrees (DD). Recovery regions are as follows: EBS—Eastern Bering Sea, NBS—North Bering Sea, RUS—Russian waters, and WGOA—Western Gulf of Alaska. Asterisk indicates physically recovered tag. NA for barotrauma recovery time (“barotr”) indicates time series data were too sparse to determine.

*Physically recovered tag.

†Captured by Russian fishing vessel.

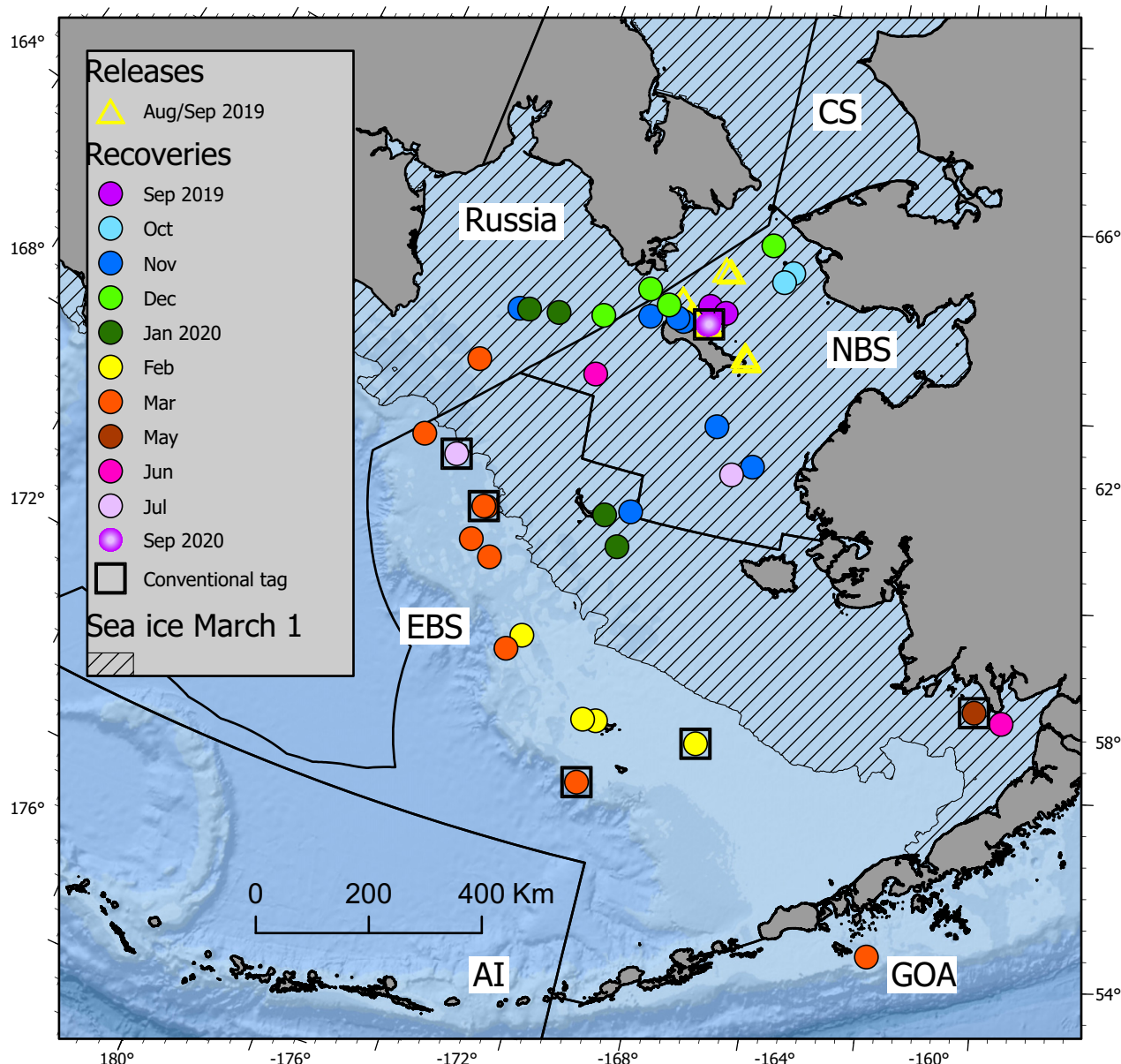
‡Mortality under sea ice.

Table 2. Conventional tag recoveries from the September 2019 release tagging platform at the Native Village of Savoonga.

| Tag ID | Rel date | Rel lat | Rel long | Depth (m) | Length (cm) | Rec date | Rec lat | Rec long | Rec region | Days at liberty |
|--------|----------|---------|----------|-----------|-------------|-----------|---------|----------|------------|-----------------|
| 308518 | 9/9/2019 | 63.751 | -170.311 | 42 | 60 | 2/8/2020 | 57.233 | -167.674 | EBS | 151 |
| 308530 | 9/9/2019 | 63.753 | -170.329 | 42 | 78 | 3/21/2020 | 56.212 | -170.778 | EBS | 193 |
| 308563 | 9/9/2019 | 63.752 | -170.277 | 41 | 68 | 3/21/2020 | 59.983 | -175.833 | EBS | 193 |
| 308584 | 9/9/2019 | 63.753 | -170.284 | 41 | 61 | 5/17/2020 | 58.352 | -159.575 | EBS | 250 |
| 308504 | 9/9/2019 | 63.751 | -170.311 | 42 | 63 | 7/13/2020 | 60.621 | -177.216 | EBS | 307 |
| 308569 | 9/9/2019 | 63.752 | -170.277 | 41 | 71 | 9/9/2020 | 63.752 | -170.277 | NBS | 365 |

Note: A total of 86 conventional tags were released, and six tags were recovered by the commercial fishery and reported by the onboard fisheries observer. The latitude and longitude for release and recovery are shown in decimal degrees (DD). Release and recovery regions are as follows: EBS—Eastern Bering Sea, NBS—North Bering Sea, RUS—Russian waters, and WGOA—Western Gulf of Alaska.

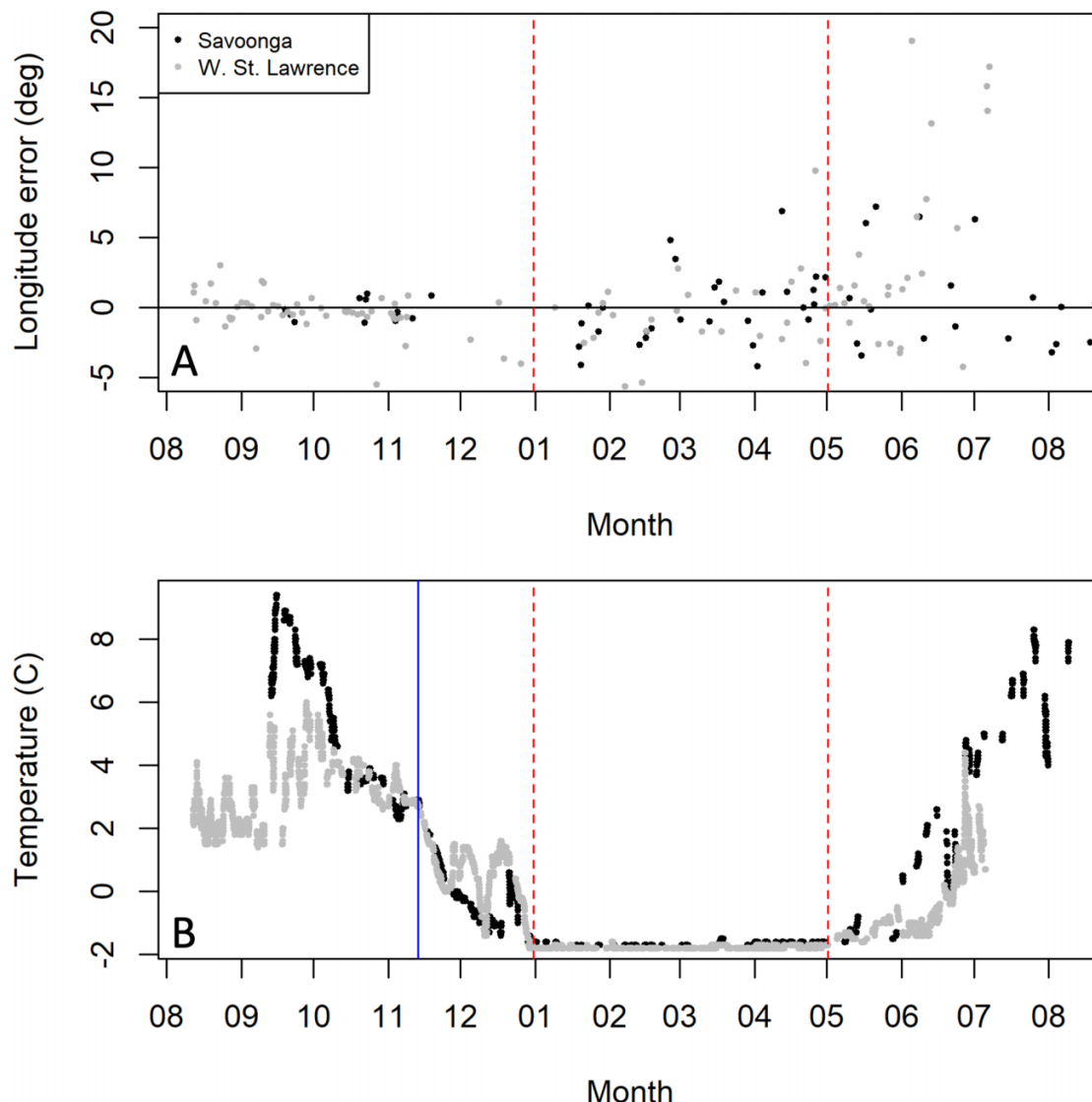
Fig. 2. Satellite and conventional tag recovery locations by month and management area (CS = Chukchi Sea, NBS = Northern Bering Sea, EBS = Eastern Bering Sea, GOA = Gulf of Alaska, and AI = Aleutian Islands). Conventional tags are indicated by a black square around the month symbol. Sea ice extent (diagonal hatched lines) is shown for 1 March 2020 (U.S. National Ice Center 2010). Base map: ArcGIS World Ocean Base (ESRI 2011). Map projection: Albers Equal Area Conic, UTM. Map datum: NAD 1983.



PSATs (21%) reported earlier than the scheduled pop-up date (due to mortality or tag shedding) after deployments ranging from 134 to 303 days. One PSAT (Tag 184060) was attached to a fish that died within a day of being covered by sea ice (based on unchanging depth observations after bottom temperatures reached -1.8°C) and popped up under the sea ice on its scheduled pop-up date in March. It was carried north by the sea ice and began to transmit in open waters in June. Of the five tags that did not transmit to satellites, two were programmed to pop-up in the winter (December–March) and three were programmed to pop-up the following summer.

Recovery locations (i.e., pop-up locations and commercial fisheries recaptures) were located in NBS, EBS, Russian waters, and the GOA throughout the period of PSAT deployment (Fig. 2). From August through November 2019, most recovery locations were located in the NBS ($n = 9$), but recovery locations also occurred in Russian waters ($n = 1$) and the EBS ($n = 1$). During the following winter months (December 2019 through March 2020), recovery locations occurred in NBS ($n = 2$), Russian waters ($n = 3$), EBS ($n = 9$), and the GOA ($n = 1$). During the summer of 2020, three recovery locations were located in the NBS and one was observed in the Bristol Bay region of the EBS.

Fig. 3. Stationary tag light and temperature data. (A) Difference between stationary tag derived light-based longitude estimates and longitude of stationary mooring. Vertical red dashed lines indicate dates of sea ice coverage and retreat. (B) Temperature time series. Solid blue horizontal line indicates migration initiation date based on net squared displacement analyses (Supplementary Data S1).



Stationary tags provided valuable information about light-based longitude and temperature in the release location over the course of the study. The root mean square error (RMSE) of longitude estimates from August through the beginning of December was 0.76 degrees for Savoonga and 1.28 degrees for western St. Lawrence (Fig. 3A). Longitude estimates were produced even when the study area was covered by sea ice, though the precision was greatly decreased (RMSE 2.46 degrees for Savoonga and 3.76 degrees for western St. Lawrence). Temperatures during summer were warmer at the Savoonga stationary tag compared to the western St. Lawrence stationary tag (Fig. 3B). Both stationary tags experienced rapid cooling in November and then were covered by sea ice on 31 December 2019. The recorded temperature was -1.8°C under the sea ice. Sea ice began to retreat from the stationary tag locations at the beginning of May, when the temperature started to increase.

Geolocation

Movement pathways were reconstructed from PSAT data for 31 of the 33 PSATs that reported to the Argos satellites. Reconstructed pathways for all 31 fish are available in [Markowitz et al. \(2025\)](#). Diffusion estimates ranged from 4 to 146.2 km^2/day (Table 3). Reconstructed pathways provided information on movement during the summer of 2019 as well as migration pathways to and from locations occupied during the peak spawning period (Fig. 4). Of the 31 geolocated data sets, 11 provided information on summertime movement (August–November). Viterbi pathways from those reconstructed pathways indicate movement primarily within the NBS during this time (Fig. 5A). Eight of the 31 data sets had end locations during December and January and thus provided information on the migratory period (Fig. 5B), where fish began to move out of the NBS ahead of oncoming sea

Table 3. Geolocation information for all geolocated fish.

| Tag ID | Data | #Mvst | D1 | D2 |
|---------|----------|-------|-------|-----|
| 183942 | PSAT | 1 | 58 | NA |
| 183943 | PSAT | 1 | 93.2 | NA |
| 183945 | PSAT | 1 | 144.4 | NA |
| 183947 | Detailed | 1 | 51.6 | NA |
| 183948 | PSAT | 1 | 93.2 | NA |
| 183949 | Detailed | 1 | 32 | NA |
| 183950 | PSAT | 1 | 146.2 | NA |
| 183951 | PSAT | 1 | 103.4 | NA |
| 183952 | PSAT | 1 | 102.4 | NA |
| 183953 | PSAT | 1 | 16 | NA |
| 183954 | PSAT | 1 | 4 | NA |
| 183955 | PSAT | 1 | 6.4 | NA |
| 183956* | PSAT | 2 | 30 | 100 |
| 183957 | PSAT | 1 | 60.6 | NA |
| 183958 | PSAT | 1 | 36.2 | NA |
| 183959 | PSAT | 1 | 50.3 | NA |
| 183960 | PSAT | 1 | 93 | NA |
| 183961 | PSAT | 1 | 90 | NA |
| 183962 | Detailed | 1 | 48 | NA |
| 183964 | PSAT | 1 | 36.2 | NA |
| 183965 | PSAT | 1 | 144.4 | NA |
| 183968 | Detailed | 1 | 32 | NA |
| 183970 | PSAT | 1 | 144.4 | NA |
| 183971 | Detailed | 1 | 48.4 | NA |
| 184057 | PSAT | 1 | 19.6 | NA |
| 184058 | PSAT | 1 | 102.4 | NA |
| 184059 | PSAT | 1 | 129.6 | NA |
| 184060 | PSAT | 1 | 57.6 | NA |
| 184061* | PSAT | 2 | 30 | 100 |
| 184062* | PSAT | 2 | 30 | 100 |
| 184064 | Detailed | 1 | 17.2 | NA |

Note: Type of data set (PSAT = transmitted, Detailed = physically recovered), number of movement states used in the HMM, and value of diffusion used for each movement state. Fish for which diffusion was not estimated directly during geolocation are indicated by an asterisk. PSAT, pop-up satellite tag.

ice. Nine of the 31 data sets had end locations in February or March and thus provided information on presumed spawning locations (Fig. 5C), most of which (8/9) were located south and west of the extent of sea ice during that period. Three of the 31 data sets had end locations during the following spring and summer (Fig. 5D) and thus provided information on presumed spawning locations (February/March) as well as post-spawning migrations. Two of these fish began moving back toward the NBS as sea ice retreated, while one fish moved into Bristol Bay in June.

Monthly location probability composites for all tagged fish combined indicate that most tagged fish were located within the NBS through November 2019, while some likely occupied adjacent Russian waters and the northern portion of the EBS during this time (Fig. 6). With the onset of sea ice and corresponding low water temperature in the NBS in December, tagged animals began to move out of the NBS to other management regions, primarily southward to the EBS. From De-

cember 2019 through March 2020, tagged fish moved to the edge of the Bering Sea shelf ahead of the oncoming sea ice edge. Conventional tags recovered during this time were also located on the shelf edge in close proximity to satellite-tagged fish.

During the peak spawning period, February 15 to March 31, the majority (77.1% of the total location probability for all fish combined, roughly equivalent to 9 tagged fish) of the 12 tagged fish still at liberty were located along the EBS shelf edge (Fig. 7) in traditional spawning areas (Neidetcher et al. 2014). However, some fish were likely located in Russian waters (16.3% of the total location probability for all fish combined; roughly equivalent to 2 fish) and the GOA (6.6% of the total location probability for all fish combined; roughly equivalent to 1 fish) during this time. Location probability estimated for the NBS during the peak spawning period was infinitesimal (0.02% of the total location probability for all fish combined), and no probability was observed in the Aleutian Islands region.

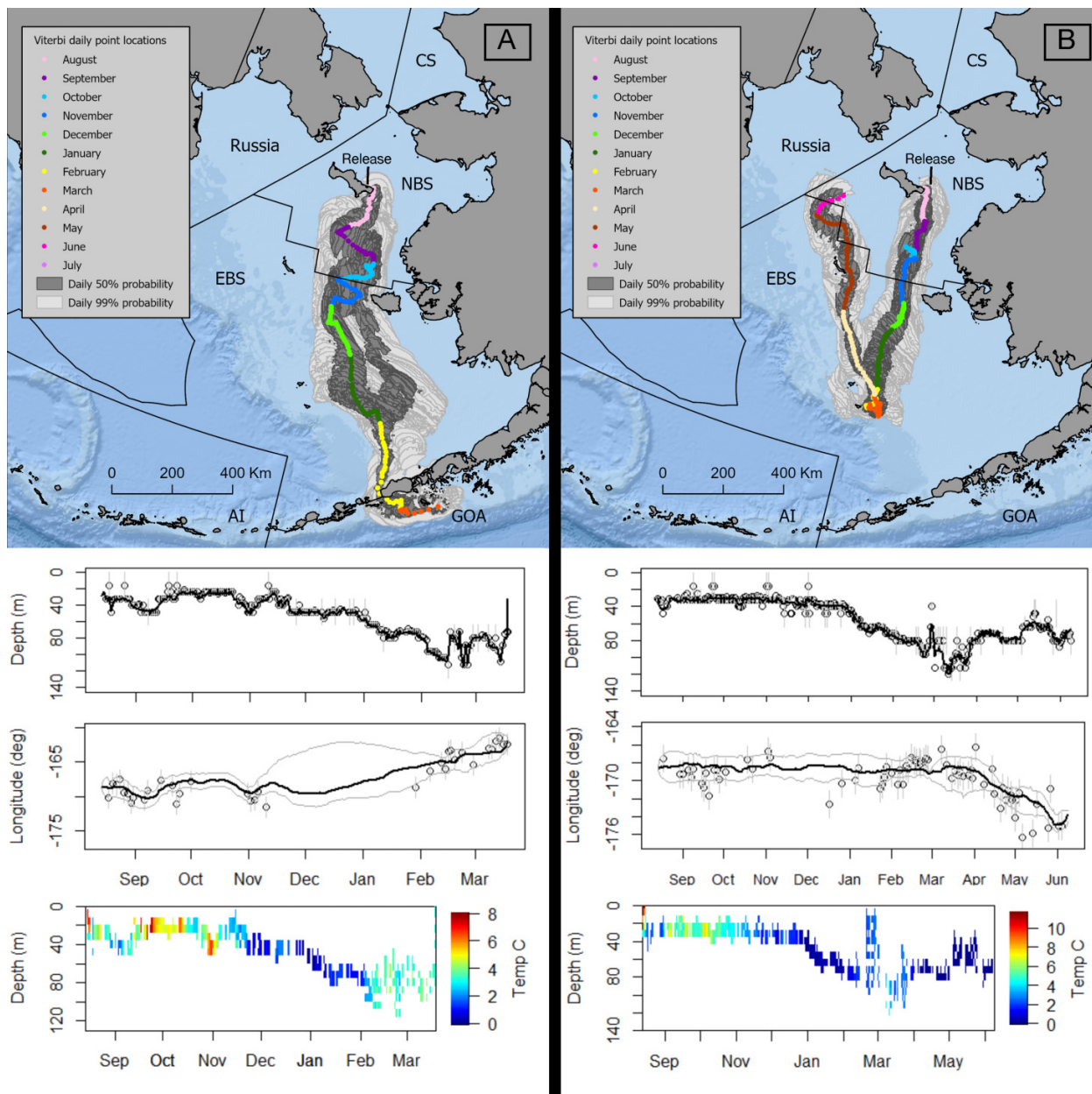
Inference from composite probabilities was limited after March 2020, as only 3 geolocated fish remained at large. Two geolocated fish moved north and east toward the NBS following the winter months as the sea ice retreated, while 1 fish moved east to the Bristol Bay region of the EBS in June. A conventional tag was also recovered in Bristol Bay in May. In all, 4 tagged fish were present in the NBS the following summer: 2 geolocated fish that returned to the NBS by June or July, a PSAT pop-up in July that did not provide enough data for geolocation, and a conventional tag recapture within a few kilometers of its release location near Savoonga almost a year after it was tagged.

Monthly composite probabilities by management area indicate a steep decline in location probability in the NBS beginning in November (Fig. 8). At the same time, location probability sharply increased in the EBS to the south. Low levels of location probability were present in Russian waters year-round. Probability in the GOA appeared in March. Although sample sizes are very small, location probability did increase in the NBS again beginning in June.

Migration timing and extent

NSD analyses suggested that winter spawning migrations out of the NBS began in November. Of the 17 fish with pop-up dates later than 1 January 2020, 10 fish had migration movement patterns described by a logistical curve with asymptote, mid-point, and scale parameters (Supplementary Data S1). These 10 data sets were used to estimate migration extent and timing for the tagged fish population using a mixed effects model. The asymptote is interpreted as the squared distance traveled to winter spawning areas, while the mid-point of the logistical curve and the scale parameter together determine the migration initiation date. The best-fitting model featured a random asymptote and first order autocorrelation. The population asymptote (fixed effect) was estimated to be 600 289 sq km (s.e. 124 453) corresponding to an average distance moved to spawning areas of 775 km (95% C.I. 597–919 km). The square root of estimated individual asymptotes (random

Fig. 4. Examples of reconstructed movement paths for two Pacific cod illustrate (A) movement from the Northern Bering Sea to a spawning area in the Gulf of Alaska (tag 183950), and (B) movement from the Northern Bering Sea to the Eastern Bering Sea to spawn, followed by a return to Northern Bering Sea the following summer (tag 183948). Below each reconstructed pathway are plots of maximum daily depth and longitude used as inputs to the geolocation model (observations are hollow circles with vertical gray lines that indicate measurement uncertainty, black line is model-estimated depth or longitude, and light gray horizontal lines for longitude indicate the daily minimum and maximum longitude from the 99% error polygons). Temperature-depth profiles (average daily temperature in 8 m depth bins) indicate temperatures experienced by tagged fish over the course of the tagging period. Base map: ArcGIS World Ocean Base (ESRI 2011). Map projection: Albers Equal Area Conic, UTM. Map datum: NAD 1983.

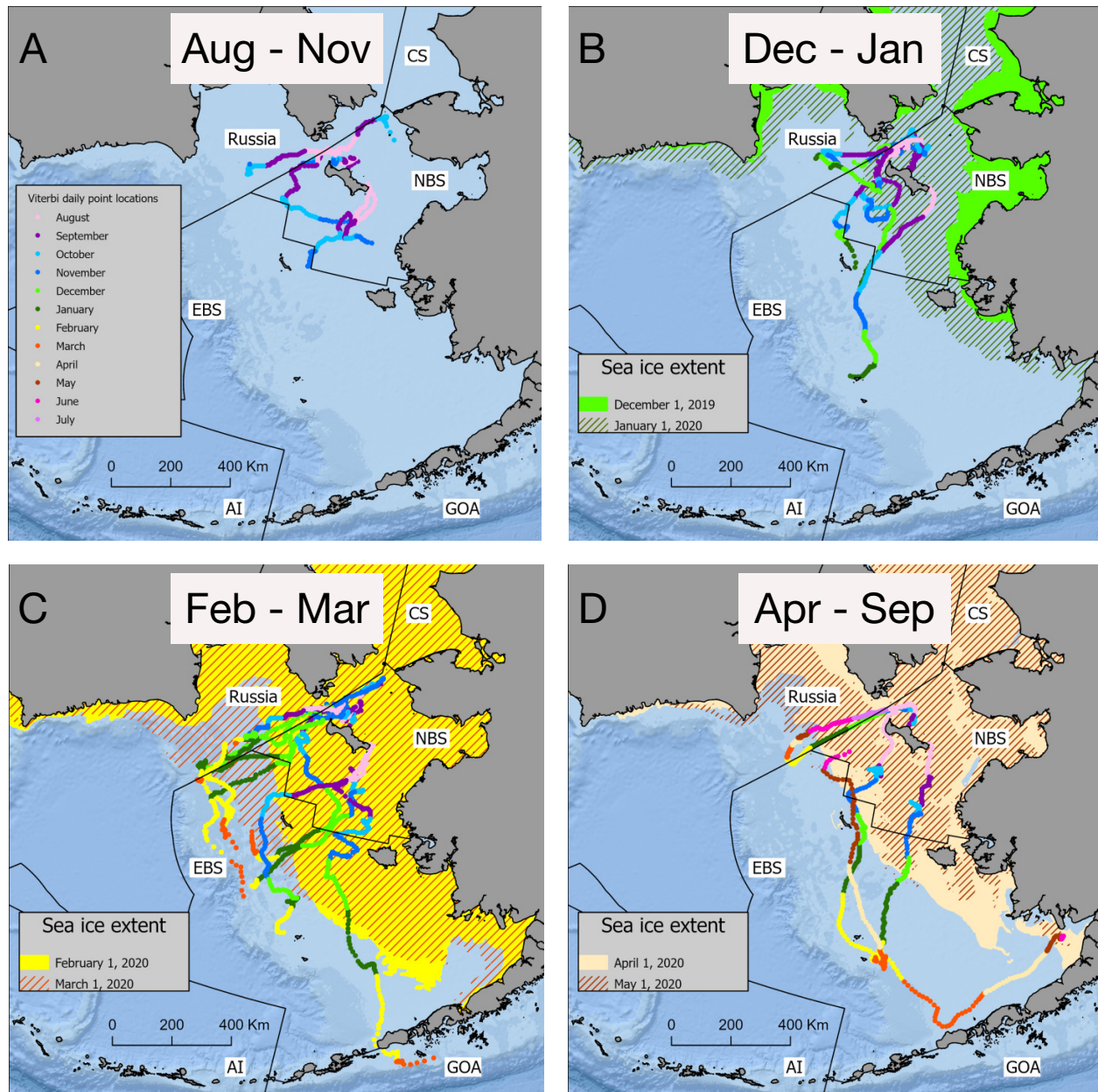


effect) ranged from 464 to 1166 km. The random effects standard deviation was 386,818 sq km, corresponding to 622 km. Estimates for θ and φ were 181 days (s.e. 1.7) and 25.8 (s.e. 1.2), which correspond to a migration initiation date of November 12 (95% C.I. November 2 to November 23). The autocorrelation coefficient was 0.997.

PSAT depth and temperature data

Changes in maximum daily depth provided an overall indication of seasonal movement out of the NBS. The monthly model performed better than the null (intercept-only) or seasonal models (Table 4), where all months were significantly

Fig. 5. Reconstructed Pacific cod movement paths (Viterbi daily location estimates) for satellite tags recovered (A) August–November, (B) December–January, (C) February–March, and (D) April–September 2020. Sea ice extent (colored or diagonal hatched line polygons) is shown during winter months and is not present during summer months (U.S. National Ice Center 2010). Base map: ArcGIS World Ocean Base (ESRI 2011). Map projection: Albers Equal Area Conic, UTM. Map datum: NAD 1983.



different ($p < 0.05$). The standard deviation of random effects (Tag ID) was 13.9 m. Fixed-effect estimates of maximum daily depth from August to November were less than 65 m, corresponding to maximum depths present on the NBS shelf (Fig. 9A). Beginning in December, depth began to increase as fish moved to the shelf edge in the winter. The deepest maximum daily depths were observed in March, the peak spawning month, followed by a return to shallower depths in the spring.

Monthly trends in maximum and minimum temperatures reflected a range of thermal habitats occupied dur-

ing the summer. Monthly models performed better than null (intercept-only) or seasonal models for both minimum and maximum temperatures (Table 4). For the maximum daily temperature mixed-effects model, all months but June ($p = 0.37$) were significantly different from the August intercept ($p < 0.05$). The standard deviation of random effects (Tag ID) was 1.19°C . For the minimum daily temperature mixed-effects model, all months but November ($p = 0.63$) and June ($p = 0.55$) were significantly different from the August intercept ($p < 0.05$). The standard deviation of random effects (Tag ID) was 0.95°C .

Fig. 6. Monthly composite location probability for satellite tagged Pacific cod from August 2019 to June 2020. The number of tagged animals that comprise each probability surface is provided for each month. Conventional tag recaptures during each month are indicated by green stars. Sea ice coverage (diagonal hatched lines) is shown during winter months and is not present during summer months (U.S. National Ice Center 2010). Base map: ArcGIS World Ocean Base (ESRI 2011). Map projection: Albers Equal Area Conic. UTM. Map datum: NAD 1983.

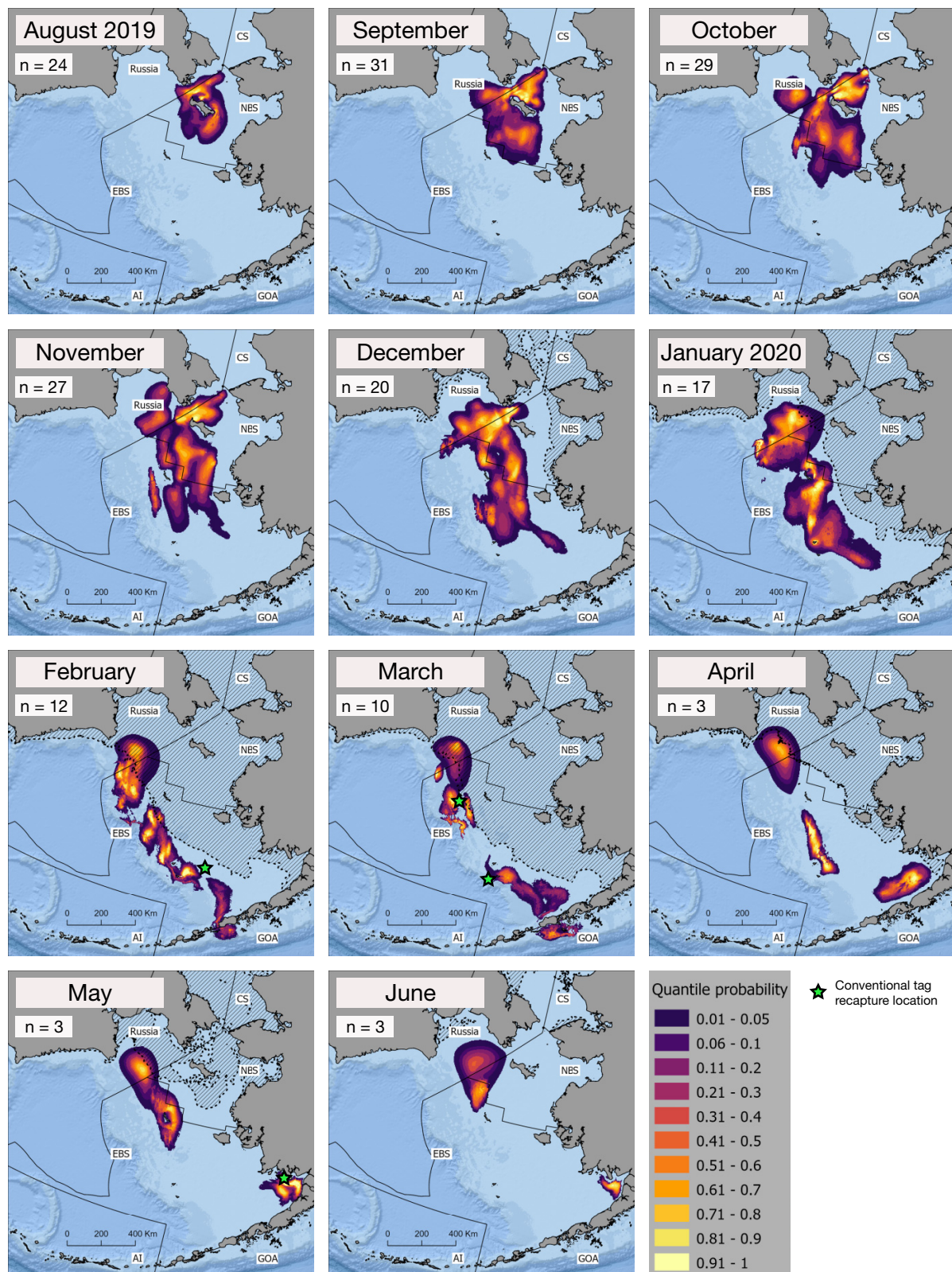
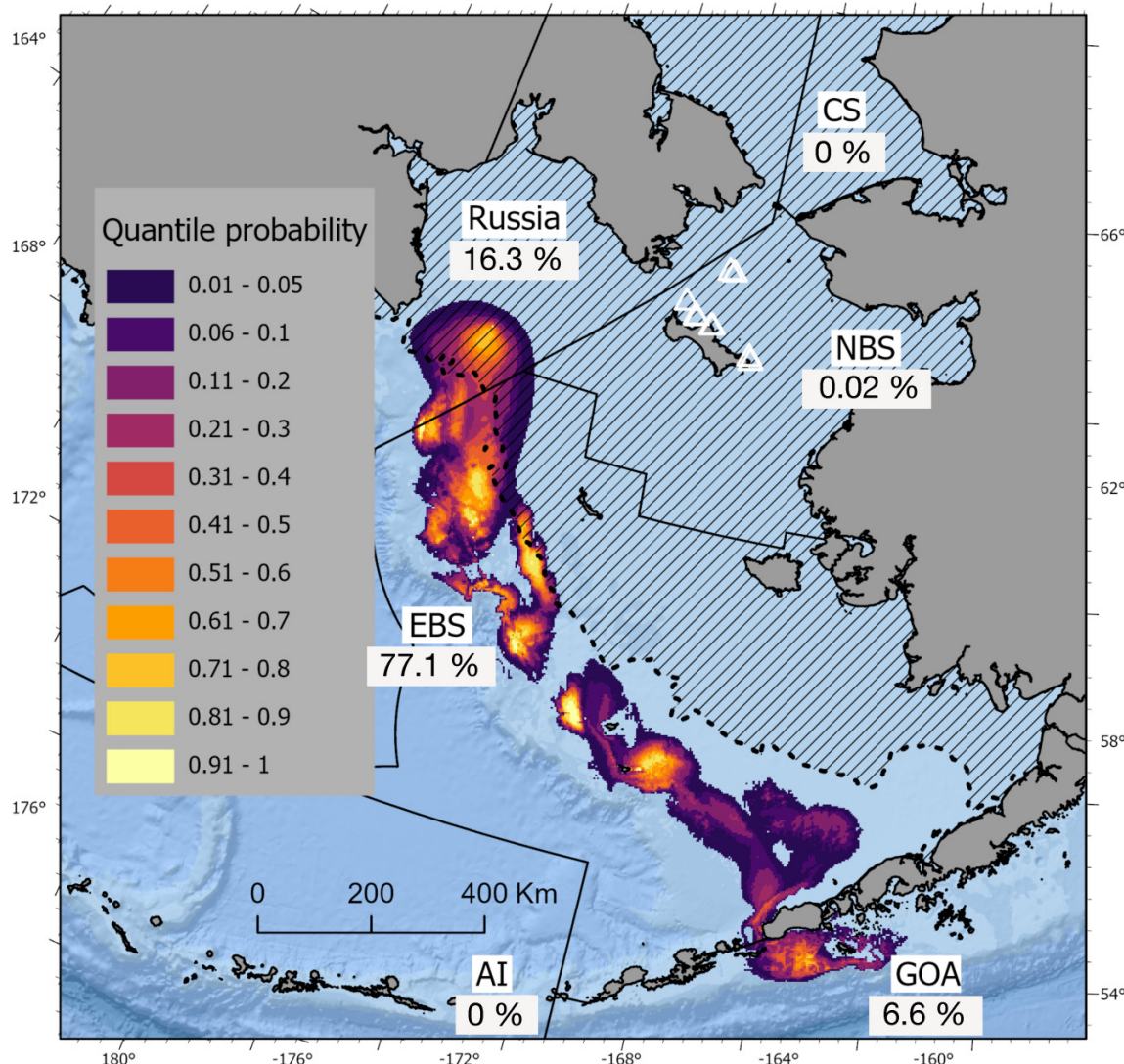


Fig. 7. Composite location probability of Pacific cod during the peak spawning period (February 15 to March 31) by management region (NBS = Northern Bering Sea, EBS = Eastern Bering Sea, GOA = Gulf of Alaska, AI = Aleutian Islands). Probability composite of 12 tagged Pacific cod. August/September release locations indicated by white triangles. Sea ice extent for 15 March 2020 (U.S. National Ice Center 2010) is indicated by diagonal hatched lines. Base map: ArcGIS World Ocean Base (ESRI 2011). Map projection: Albers Equal Area Conic, UTM. Map datum: NAD 1983.



Although fixed-effect estimates ranged from 3 to 6 °C, minimum and maximum daily temperatures observed by individual fish ranged from -1.6 to 11.5 °C (Fig. 9B). Temperatures experienced by the tagged fish cooled during winter as fish began to migrate (December through January) but increased again as some fish moved south into spawning areas with warmer temperatures (such as the Pribilof Canyon and the GOA). Temperatures dropped to -1 °C in April, as fish began moving away from spawning locations. Some fish occupied temperatures below -1 °C for extended periods of time.

Discussion

Seasonal movement

This study provided the first detailed observations of Pacific cod movement from summer foraging to winter spawn-

ing areas in the Bering Sea. Reconstructed pathways generated by the HMM provided important insights into migration characteristics and presumed winter spawning areas of Pacific cod tagged in the NBS during the summer foraging period. We found no evidence that any satellite-tagged fish remained in the NBS through the winter. Instead, most tagged fish migrated to traditional spawning areas in the EBS. The location probability distribution and depth range distribution of satellite-tagged fish from mid-February through March largely aligned with mapped locations and depth distributions of spawning fish along the Bering Sea shelf break and into the western GOA (Neidetcher et al. 2014). However, we found that some tagged fish were located farther north along the shelf break in Russian waters, where Neidetcher et al. were unable to sample. We also observed some seasonal movement to the GOA, which suggests a previously unknown

Fig. 8. Monthly composite Pacific cod location probabilities (see Fig. 6) by management region (NBS = Northern Bering Sea, EBS = Eastern Bering Sea, GOA = Gulf of Alaska).

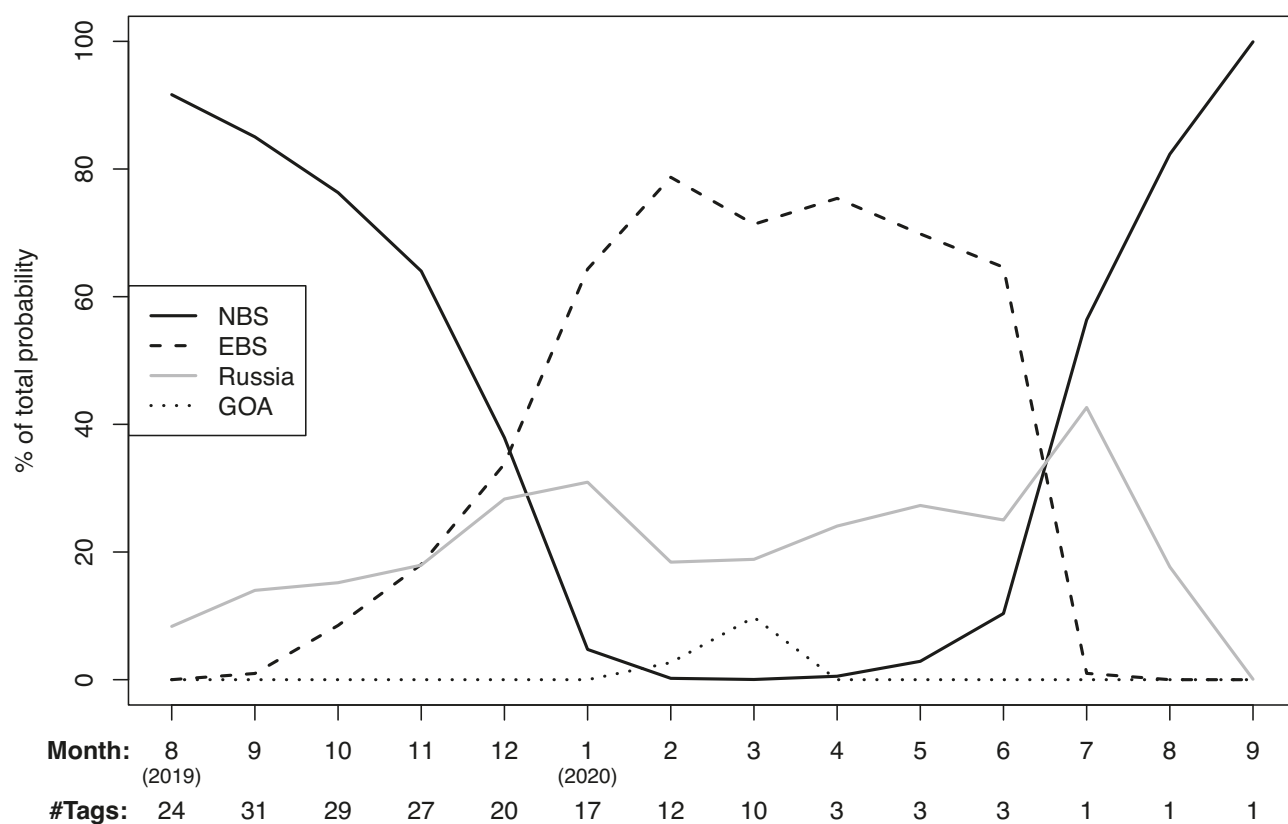


Table 4. Depth and temperature mixed-effects model Akaike information criterion (AIC) values and degrees of freedom (df) for model selection.

| | AIC | df |
|----------------------------|--------|----|
| Maximum depth | | |
| Null | 25 929 | 3 |
| Seasonal | 27 152 | 4 |
| Monthly | 24 589 | 13 |
| Maximum temperature | | |
| Null | 9284 | 3 |
| Seasonal | 8825 | 4 |
| Monthly | 8443 | 13 |
| Minimum temperature | | |
| Null | 8732 | 3 |
| Seasonal | 8306 | 4 |
| Monthly | 7894 | 13 |

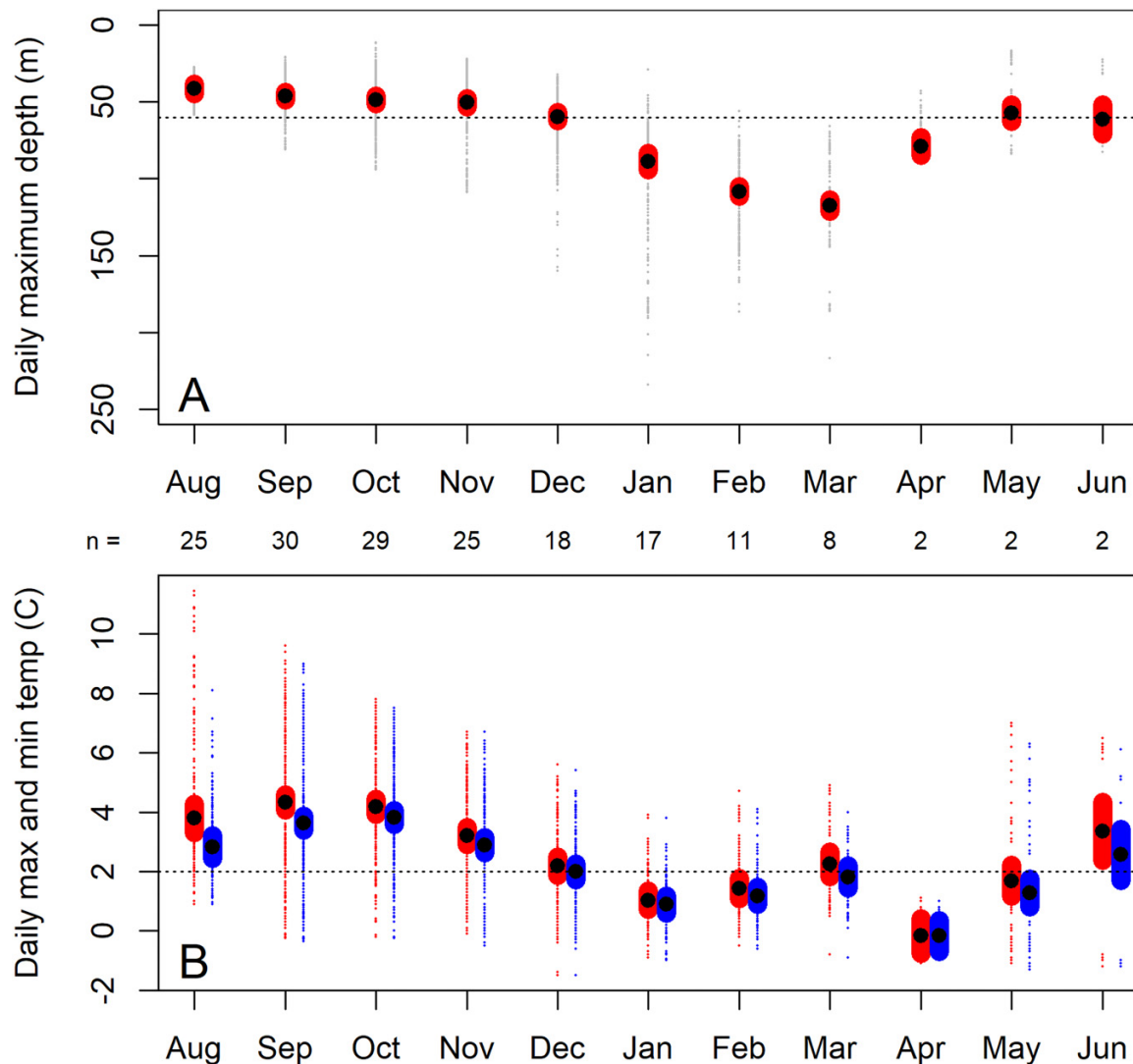
Note: All mixed-effects models were fit using maximum likelihood for model comparisons. Null = intercept only, seasonal = winter (December–March) or summer (April–November).

degree of connectivity between foraging areas in the NBS and GOA spawning areas.

Like previous Pacific cod tagging studies, our study demonstrates that Pacific cod can conduct large-scale seasonal migrations between summer foraging and winter spawning locations. A satellite tagging study on Pacific cod in the Aleutian

Islands found that tagged cod migrated up to 344 km from winter spawning to summer foraging locations, where fish remained within the Aleutian Island management area (Bryan et al. 2021). A conventional tagging study conducted in the EBS between 1982 and 1990 demonstrated southward movement from summer to winter, including movement from the EBS into the western GOA (Shimada and Kimura 1994). Distances moved of up to 1000 km were observed in that study; however, most winter recaptures occurred at distances between 200 and 500 km from summertime release locations. Another conventional tagging study conducted on Bering Sea spawning grounds in the winter observed northward movement of up to 400 km between winter spawning and summer foraging areas (Rand et al. 2014). Our study reports a twofold increase in migration distances for fish tagged in the NBS compared to these previous studies, with an estimated migration extent of 775 km. This may reflect increased travel distances needed to reach optimal spawning habitats, e.g., areas with bottom temperatures between 4 and 6 °C (Laurel and Rogers 2020). The differences in migration extent from the previous EBS tagging studies could also be related to the difference in precision provided by reconstructed pathways compared to location-only conventional tag recoveries. Typically, conventional tag recoveries are aggregated over several months, years, and recovery regions, and are spatially limited by the seasonal distribution of commercial fishing effort.

Fig. 9. Daily depth and temperature data from satellite tagged Pacific cod summarized by month. (A) Daily maximum depth observations (gray points) and mixed-effects model population mean estimate (black point) with 95% confidence intervals (red). Horizontal dotted line depicts the 90% quantile depth of the Northern Bering Sea management area. (B) Daily maximum (red points) and minimum temperature (blue points) and mixed-effects model population means estimate (black points) with 95% confidence intervals (red and blue lines). Horizontal dotted line indicates temperature that defines the Bering Sea cold pool. Number (n) of individual tagged fish included in each month is displayed between the figures and applies to both figures.



In addition to providing information about tagged fish locations during the peak spawning period, reconstructed pathways provided information on year-round movement patterns such as partial migration and return migration. Partial migration, where a portion of the population does not conduct seasonal migrations, has been observed for Pacific cod from satellite, acoustic telemetry, and conventional tags (Rand et al. 2014; Lewandoski et al. 2018; Bryan et al. 2021) and for Atlantic cod from acoustic telemetry studies (Strøm et al. 2023). We did not observe any tagged fish to reside in the NBS shelf year-round, likely due to temperatures underneath the sea ice on the shallow shelf that are too cold for survival (see below discussion on depth and temperature). However, we did observe some tagged fish return to the NBS the follow-

ing summer after moving to other areas during the winter, indicating potential fidelity to summer foraging areas. Information on return migration is extremely difficult to obtain with conventional tags, as a fish recaptured in the release area a year later could have migrated out of the area in the winter and returned (e.g., Fig. 4B) or remained in the area year-round. Return migration to spawning areas has been observed in Atlantic cod for both acoustic telemetry and satellite tagging studies (Strøm et al. 2023; Rose and Rowe 2024). For Pacific cod, return migration to both winter spawning and summer foraging areas is a focus for future research.

Our work contributes to a growing body of research that uses PSATs to obtain detailed, fishery-independent information about large-scale seasonal movement patterns of cod

species. The first satellite-tagging study on Pacific cod provided insights into post-spawning migrations in the Aleutian Islands (Bryan et al. 2021) and established methods for Pacific cod geolocation in North Pacific waters (Nielsen et al. 2023b). A satellite tagging study on Atlantic cod in Newfoundland and Labrador used depth, temperature, and light-based longitude to demonstrate re-establishment of historical migration routes following rebound of the stock and to link migration timing to temperature and the presence of capelin, an important prey species (Rose and Rowe 2024). PSATs have also been deployed on Atlantic cod in Icelandic waters, where they have provided detailed information on swimming behavior and temperature and depth preferences (Nielsen et al. 2023a).

Relationships with temperature and sea ice

From August through the beginning of November, tagged Pacific cod remained largely within the NBS and nearby Russian waters, presumably to forage. Temperatures recorded by tagged Pacific cod during these months support observations that Pacific cod tend to occupy habitats with a broad range of temperatures warmer than 0 °C during the summer months based on trawl survey data in the EBS and NBS (Baker 2021). This finding is consistent with an expansion of Pacific cod foraging range northward during warmer years such as 2019, where a larger proportion of the NBS had bottom temperatures warmer than 0 °C (Baker 2021) compared to colder years (Rohan et al. 2022). Insights into the amount of time spent foraging in the NBS from the reconstructed pathways will be important for understanding the potential effects of predation pressure on commercially valuable benthic resources such as juvenile snow crab, a primary food item for Pacific cod (Szwalbski et al. 2023).

Winter spawning migration timing was likely related to seasonal changes in temperature and sea ice coverage. Movement to winter spawning areas was estimated by NSD analyses to begin in mid-November in conjunction with dropping temperatures that preceded sea ice coverage in the area (Fig. 3). Therefore, rapidly declining temperatures may serve as a cue for fish to leave summer foraging areas on the shallow NBS shelf. The movement of tagged fish south and west toward the shelf edge ahead of expanding sea ice from December through February (Fig. 6) suggests that the timing of migration may also be related to the timing of sea ice advance as fish respond to colder temperatures associated with sea ice expansion.

It is possible that the seawater temperature recorded by the stationary tags (−1.8 °C) underneath the sea ice on the shallow NBS shelf is too cold for Pacific cod survival when ice crystals are present. One fish that remained under the sea ice until its pop-up date likely died on the day of sea ice coverage in December based on depth and temperature data. Ongoing research on the antifreeze protein level of Pacific cod plasma suggests some individuals may be able to survive water temperatures down to about −1.3 °C in the presence of ice crystals, but not colder (C. Cheng, University of Illinois, Urbana-Champaign, pers. comm.). Antifreeze proteins have also been observed in Atlantic cod that occupy waters with

subzero temperatures, with plasma freezing points as low as −1.3 °C (Goddard et al. 1994). Therefore, if Pacific cod avoid the cold temperatures associated with sea ice coverage due to their physiological vulnerability to ice crystals and freezing, the timing and extent of annual sea ice formation in the NBS may be very important for understanding and predicting migration timing and extent.

Following the spawning period, tagged fish began movement to summer foraging areas. The colder temperatures encountered during post-spawning migrations (as cold as −1.2 °C) compared to minimum temperatures observed during summer foraging (minimum temperature −0.5 °C from August through November) could provide insights into what temperatures may be a barrier to movement versus temperatures that are typically experienced during summer foraging.

Satellite tagging in high latitudes

Our study has provided important information on the performance of satellite tags deployed through the winter in high-latitude study areas where seasonal sea ice was present. The use of satellite tags was necessary for this study because the presence of sea ice in the winter prevents the commercial fishing effort needed to provide conventional tag recaptures as well as surveys that could provide information on winter fish distributions. The relatively high amount of information received (33 of 38 tag recovery locations and reconstructed pathways for 31 of 38 tagged fish) indicates that satellite tags can reliably record data for up to a year in northern latitudes. Winter sea ice coverage did not seriously affect satellite tag pop-up rates or transmissions, largely due to the movement of tagged fish to ice-free areas during winter. Of the 5 tags that did not contact the ARGOS satellite network, only two were programmed to pop up in the winter where ice could possibly have hindered transmission. However, one tag successfully transmitted following a premature release where it was lodged under the sea ice until the sea ice retreated. Therefore, it appears that Wildlife Computers MiniPAT satellite tags can effectively store and transmit data even if the tags pop up under the sea ice.

Caveats

A number of caveats accompany the interpretation of results provided in this study. First, as is common in satellite tagging studies due to the high expense of the tags (approximately \$4000 USD), PSAT sample sizes are relatively small. Additionally, sample sizes further decreased over time as various pop-up dates were reached or tagged fish were caught. Second, location of spawning areas is inferred from tagged fish locations during the time of peak spawning rather than direct knowledge of fish spawning activity. Third, gaps in geolocation data can lead to increased daily location uncertainty estimates. However, our analysis methods for movement between management areas explicitly accounted for uncertainty in location estimates by using the entire daily probability surfaces for each fish. Fourth, the use of one or two movement states to describe movement of tagged fish is a simplification of the behavior of Pacific cod over the course of the year. This preserves simplicity of the movement

model, and in most cases multiple states aren't needed when environmental gradients are strong (such as the movements across depth gradients out of the NBS) and the diffusion kernel is at least large enough to accommodate the actual range of fish movement each day.

Management implications

Movement between management areas

The current management strategy of treating the EBS and NBS as the same population within a larger Bering Sea management area is supported by our data, assuming that the natal origin of tagged fish was the EBS spawning grounds. Most of the satellite-tagged Pacific cod moved from summer foraging areas in the NBS to traditional spawning areas in the EBS during the peak spawning season (February 15 to March 31). This result, when combined with a genetics study that found genetic similarities between Pacific cod sampled in the NBS during summer and at traditional spawning areas in the EBS during spawning season (Spies et al. 2020), suggests that the fish present in the NBS during the summer do not constitute a separate, northern population. Instead, the expansion of Pacific cod into northern waters during the summer surveys likely represents expanded summer foraging areas as speculated by several studies (Stevenson 2012; Stevenson and Lauth 2019).

However, the seasonal movement of some NBS fish to regions outside of the Bering Sea management area signals several potential areas of concern for management. Although seasonal connectivity between the EBS and the GOA has been previously observed by a conventional tagging study (Shimada and Kimura 1994), our study is the first to document seasonal connectivity between the NBS and the western GOA. Therefore, our work strengthens the evidence for connectivity between the Bering Sea and GOA management areas and provides an indication of the spatial scale of connectivity that is occurring. Currently, stock assessments do not account for connectivity between these management areas and observed movements between these areas is a growing stock assessment concern (Barbeaux et al. 2023). Incorporating connectivity into stock assessment will require additional tagging efforts to estimate the proportion of fish and timing of movement between areas across a range of environmental conditions.

Also of potential concern for management is the movement of Pacific cod outside of U.S. management areas. We found that approximately 20% of the NBS tagged fish location probability was in Russian waters year-round. The border between the U.S. and Russia bisects the shallow NBS shelf into areas with similar depths and (presumably) habitat types. The finding of summertime movement across the exclusive economic zone boundaries in that area was expected but remains difficult to quantify. During summer, U.S. and Russian fishery-independent trawl surveys have been combined to predict biomass estimates of Pacific cod on either side of the border (O'Leary et al. 2022). However, this study has provided the first evidence of movement into Russian waters during the winter, highlighting the need to understand seasonal

patterns in spawning stock distribution relative to international boundaries.

Implications for a changing climate

The northward shift of Pacific cod into the NBS during the years 2017–2019 is strongly correlated to increased water temperature during those years. Since 2021, winters have been colder in the Bering Sea and winter sea ice and summer cold pool extents in 2022 and 2023 have returned to near normal (Siddon 2023). The summertime distribution of Pacific cod in 2022 and 2023 was similar to historical distributions during colder years, with most of the population located in the EBS (Markowitz et al. 2024). This observation highlights the sensitivity of Pacific cod summertime distributions in the Bering Sea to seasonal temperature regimes and winter sea ice extent.

Although recent temperature conditions and sea ice extent in the Bering Sea have been closer to average, Arctic sea ice is forecasted to decline by most climate projections (IPCC 2023) and conditions like those of 2018 where the NBS remained nearly ice-free over winter (Stabeno and Bell 2019) are expected to become more prevalent. The resulting northward shifts in Pacific cod distribution would be expected to increase predation pressure on important subarctic invertebrate resources such as snow crab in the summer. In addition, if sea ice is absent in the winter, the NBS could potentially support a persistent Pacific cod population that not only forages but spawns in the NBS. A northward shift in optimal winter spawning habitat (Bigman et al. 2023) could potentially shorten seasonal migrations and reduce migration to the EBS.

Northward shifts in spawning distributions related to warming conditions have been observed for Atlantic cod (Sundby and Nakken 2008). A northward shift of spawning habitat into the NBS would be an important consideration for stock assessment scientists, given that the Bering Sea is currently managed as a single population (Barbeaux et al. 2023). Latitudinal differences in Pacific cod growth and natural mortality have been documented within its current range tied to temperature and length of the growing season (Ormseth and Norcross 2009). A northward shift would likely impact stock productivity with changes in recruitment, growth, and natural mortality that would need to be accounted for in the assessment. In addition, more of the stock would be made available to Russian fisheries, increasing the need to coordinate management of this stock between the United States and Russia.

Our results point to the need for adaptive management strategies to address issues related to northward shifts in distribution under different temperature regimes. The detailed data provided by this study on migration timing, pathways, and spawning or foraging areas and how those could change under different environmental conditions is valuable for development of management strategy evaluations (MSEs), an important component of adaptive management strategies (Bell et al. 2020). In turn, MSEs will inform adaptive management strategies that can incorporate cross-boundary move-

ments of a commercially exploited fish, quota setting, and other adaptive management actions (Bahri et al. 2021).

Conclusions

We found that satellite tags were an effective and essential tool for studying the seasonal movement of Pacific cod in the NBS. Our results suggest that the observed northward shift in distribution of Pacific cod into the NBS during 2017–2019 was likely related to an expansion of summer foraging grounds for EBS Pacific cod during warm years rather than the establishment of a separate, year-round NBS population. The results also provide new evidence of connectivity between the GOA, the Bering Sea, and Russian waters. Such detailed information on seasonal connectivity is important for stock identification, stock assessment, and the development of management tools that can accommodate changing environmental conditions. Continued tagging across varying temperature regimes is needed to understand the consistency of observed seasonal movement patterns and potential impact of warming ocean conditions on Pacific cod population distributions.

Acknowledgements

We thank the Siberian Yupik people from the Native Village of Savoonga for lending their knowledge and support to this project. We thank captain Richmond Toolie and crew of the F/V Scarlett, captain Perry Pungowiyi and crew of the F/V Adeline, Orville Toolie, and Savoonga fish processing plant employees for assistance with tagging. We also thank our collaborators at the Norton Sound Economic Development Corporation for assistance with the Savoonga tag release; Dawn Wehde facilitated connections with the Native Village of Savoonga and assisted with Savoonga tag deployments; Wes Jones and Myra Scholz provided logistical assistance. We thank the captain and crew of the F/V Vesteraalen and the F/V Alaska Knight for assistance and support during the Alaska Fisheries Science Center Bering Sea survey tag releases. We thank the following NOAA Alaska Fisheries Science Center employees for their support of the project: Rebecca Haehn and Duane Stevenson helped with tagging efforts during the Bering Sea survey. Ingrid Spies, Cecilia O’Leary, and Steve Barbeaux aided with experimental design. Bianca Prohaska, Sean Rohan, and Ben Laurel provided analysis support and review of earlier versions of the manuscript. We are grateful for the input from two anonymous reviewers who provided valuable feedback and suggestions for the manuscript. Pacific cod Harvesters provided general support and assistance with tag recoveries. We thank Kenny Down and John Gauvin for the inspiration and support of the Pacific cod cooperative tagging program.

Article information

History dates

Received: 30 October 2024

Accepted: 24 July 2025

Accepted manuscript online: 7 August 2025

Version of record online: 24 September 2025

Copyright

© 2025 Authors Nielsen and Rand. Permission for reuse (free in most cases) can be obtained from copyright.com.

Data availability

Data and code used for analyses are available at <https://doi.org/10.6084/m9.figshare.29817218>.

Author information

Author ORCIDs

Julie K. Nielsen <https://orcid.org/0000-0002-8384-4158>

Kimberly M. Rand <https://orcid.org/0000-0001-8837-1401>

Elizabeth J. Dawson <https://orcid.org/0009-0006-7142-1445>

David Bryan <https://orcid.org/0000-0002-3846-1553>

Stan Kotwicki <https://orcid.org/0000-0002-6112-5021>

Author notes

Current affiliation for Elizabeth J. Dawson is Bureau of Ocean Energy Management, 45600 Woodland Rd, Sterling, VA 20166, USA.

Current address for Daniel G. Nichol is 270 Tala Shore Dr., Port Ludlow, WA 98365, USA.

Author contributions

Conceptualization: SFM, EJD, DB, LB, SK, DGN

Data curation: JKN

Formal analysis: JKN

Funding acquisition: SFM, LB, SK

Investigation: SFM, EJD, DB, DGN

Methodology: JKN

Project administration: SFM

Software: JKN

Supervision: SFM

Visualization: JKN, KMR

Writing – original draft: JKN, SFM, KMR

Writing – review & editing: JKN, SFM, KMR, EJD, DB, LB, SK, DGN

Competing interests

The authors declare there are no competing interests.

Funding information

Funding for this project was provided by the NOAA National Cooperative Research Program, the Norton Sound Economic Development Council, and Pacific cod harvesters.

Supplementary material

Supplementary data are available with the article at <https://doi.org/10.1139/cjfas-2024-0342>.

References

Bahri, T., Vasconcellos, M., Welch, D.J., Johnson, J., Perry, R.I., Ma, X., and Sharma, R. (Editors). 2021. Adaptive management of fisheries in response to climate change. FAO Fisheries and Aquaculture Technical Paper No. 667. FAO, Rome. doi:[10.4060/cb3095en](https://doi.org/10.4060/cb3095en).

Baker, M.R. 2021. Contrast of warm and cold phases in the Bering Sea to understand spatial distributions of Arctic and sub-Arctic gadids. *Polar Biol.* **44**: 1083–1105. doi:10.1007/s00300-021-02856-x.

Barbeaux, S.J., Barnett, L., Hall, M., Hulson, P., Nielsen, J.K., Shotwell, S.K., et al. 2023. Assessment of the Pacific cod stock in the Eastern Bering Sea. In *Plan team for groundfish fisheries of the Bering Sea and Aleutian Islands (compiler), Stock Assessment and Fishery Evaluation report for the groundfish resources of the Bering Sea and Aleutian Islands*. North Pacific Fishery Management Council.

Bell, R.J., Odell, J., Kirchner, G., and Lomonico, S. 2020. Actions to promote and achieve climate-ready fisheries: summary of current practice. *Mar. Coastal Fish.* **12**(3): 166–190. doi:10.1002/mcf2.10112.

Bigman, J.S., Laurel, B.J., Kearney, K., Hermann, A.J., Cheng, W., Holsman, K.K., and Rogers, L.A. 2023. Predicting Pacific cod thermal spawning habitat in a changing climate. *ICES J. Mar. Sci.* doi:10.1093/icesjms/fsad096.

Börger, L., and Fryxell, J. 2012. Quantifying individual differences in dispersal using net squared displacement. In *Dispersal and spatial evolutionary ecology*. Edited by J. Clobert, M. Baguette, T. Benton and J. Bullock. Oxford University Press. pp. 222–230.

Bryan, D.R., McDermott, S.F., Nielsen, J.K., Fraser, D., and Rand, K.M. 2021. Seasonal migratory patterns of Pacific cod (*Gadus macrocephalus*) in the Aleutian Islands. *Anim. Biotelemetry*, **9**. doi:10.1186/s40317-021-00250-2.

Bunnefeld, N., Börger, L., van Moorter, B., Rolandsen, C.M., Dettki, H., Solberg, E.J., and Ericsson, G. 2011. A model-driven approach to quantify migration patterns: individual, regional and yearly differences. *J. Anim. Ecol.* **80**(2): 466–476. doi:10.1111/j.1365-2656.2010.01776.x. PMID: 21105872.

Campana, S.E., Stefánsdóttir, R.B., Jakobsdóttir, K., and Sólmundsson, J. 2020. Shifting fish distributions in warming sub-Arctic oceans. *Sci. Rep.* **10**(1): 16448. doi:10.1038/s41598-020-73444-y. PMID: 33020548.

Danielson, S.L., Dobbins, E.L., Jakobsson, M., Johnson, M.A., Weingartner, T.J., Williams, W.J., and Zarayskaya, Y. 2015. Sounding the northern seas. *Eos*, **96**. doi:10.1029/2015EO040975.

ESRI. 2011. World Ocean Base. Sources: Esri, GEBCO, NOAA, Garmin, and other contributors.

Goddard, S.V., Wroblewski, J.S., Taggart, C.T., Howse, K.A., Bailey, W.L., Kao, M.H., and Fletcher, G.L. 1994. Overwintering of adult Northern Atlantic cod (*Gadus morhua*) in cold inshore waters as evidenced by plasma antifreeze glycoprotein levels. *Can. J. Fish. Aquat. Sci.* **51**(12): 2834–2842. doi:10.1139/f94-282.

Intergovernmental Panel on Climate Change. 2023. Ocean, cryosphere and sea level change. In *Climate Change 2021 – The Physical Science Basis: Working Group I Contribution to the Sixth Assessment Report of the Intergovernmental Panel on Climate Change*. Cambridge University Press, Cambridge. pp. 1211–1362.

Laurel, B.J., and Rogers, L.A. 2020. Loss of spawning habitat and prerecruits of Pacific cod during a Gulf of Alaska heatwave. *Can. J. Fish. Aquat. Sci.* **77**(4): 644–650. doi:10.1139/cjfas-2019-0238.

Le Bris, A., Frechet, A., and Wroblewski, J.S. 2013. Supplementing electronic tagging with conventional tagging to redesign fishery closed areas. *Fish. Res.* **148**: 106–116. doi:10.1016/j.fishres.2013.08.013.

Levine, R.M., De Robertis, A., Grünbaum, D., Wildes, S., Farley, E.V., Stabeno, P.J., and Wilson, C.D. 2023. Climate-driven shifts in pelagic fish distributions in a rapidly changing Pacific Arctic. *Deep Sea Res. Part II*, **208**: 105244. doi:10.1016/j.dsdr.2022.105244.

Lewandoski, S.A., Bishop, M.A., and McKinzie, M.K. 2018. Evaluating Pacific cod migratory behavior and site fidelity in a fjord environment using acoustic telemetry. *Can. J. Fish. Aquat. Sci.* **75**(11): 2084–2095. doi:10.1139/cjfas-2017-0432.

Markowitz, E.H., Dawson, E.J., Charriere, N.E., Prohaska, B.K., Rohan, S.K., Stevenson, D.E., and Britt, L.L. 2022. Results of the 2019 eastern and northern Bering Sea continental shelf bottom trawl survey of groundfish and invertebrate fauna. NOAA technical memorandum NMFS-AFSC. 451. doi:10.25923/d641-xb21.

Markowitz, E.H., Dawson, E.J., Wassermann, S.N., Anderson, C.B., Rohan, S.K., Charriere, N.E., and Stevenson, D.E. 2024. Results of the 2023 eastern and northern Bering Sea continental shelf bottom trawl survey of groundfish and invertebrate fauna. U.S. Department of Commerce, NOAA technical memorandum NMFS-AFSC-587.

Markowitz, E.H., Rand, K.M., Bryan, D., Dawson, L., Dowlin, A., Levy, C., et al. 2025. Pacific cod satellite tagging results from the Bering Sea summer 2019 deployments. U.S. Department of Commerce, NOAA Technical Memorandum NMFS-AFSC-497, 51p.

Mueter, F.J., and Litzow, M.A. 2008. Sea ice retreat alters the biogeography of the Bering Sea continental shelf. *Ecol. Appl.* **18**(2): 309–320. doi:10.1890/07-0564.1. PMID: 18488598.

Neidetcher, S.K., Hurst, T.P., Ciannelli, L., and Legerwell, E.A. 2014. Spawning phenology and geography of Aleutian Islands and eastern Bering Sea Pacific cod (*Gadus macrocephalus*). *Deep Sea Res. Part II*, **109**: 204–214. doi:10.1016/j.dsdr.2013.12.006.

Nichol, D., Honkalehto, T., and Thompson, G. 2007. Proximity of Pacific cod to the sea floor: using archival tags to estimate fish availability to research bottom trawls. *Fish. Res.* **86**(2-3): 129–135. doi:10.1016/j.fishres.2007.05.009.

Nichol, D.G., and Chilton, E.A. 2006. Recuperation and behaviour of Pacific cod after barotrauma. *ICES J. Mar. Sci.* **63**: 83–94. doi:10.1016/j.icesjms.2005.05.021.

Nielsen, A., and Sibert, J.R. 2007. State-space model for light-based tracking of marine animals. *Can. J. Fish. Aquat. Sci.* **64**(8): 1055–1068. doi:10.1139/f07-064.

Nielsen, J., Estévez-Barcia, D., Post, S., Christensen, H.T., Retzel, A., Meire, L., et al. 2023a. Validation of pop-up satellite archival tags (PSATs) on Atlantic cod (*Gadus morhua*) in a Greenland fjord. *Fish. Res.* **266**. doi:10.1016/j.fishres.2023.106782.

Nielsen, J.K., Bryan, D.R., Rand, K.M., Arostegui, M.C., Braun, C.D., Galuardi, B., and McDermott, S.F. 2023b. Geolocation of a demersal fish (Pacific cod) in a high-latitude island chain (Aleutian Islands, Alaska). *Anim. Biotelemetry*, **11**(1): 29. doi:10.1186/s40317-023-00340-3.

Nielsen, J.K., Mueter, F., Adkison, M., McDermott, S., Loher, T., and Seitz, A.C. 2019. Effect of study area bathymetric heterogeneity on parameterization and performance of a depth-based geolocation model for demersal fish. *Ecol. Model.* **402**: 18–34. doi:10.1016/j.ecolmodel.2019.03.023.

O’Leary, C.A., DeFilippo, L.B., Thorson, J.T., Kotwicki, S., Hoff, G.R., Kullik, V.V., et al. 2022. Understanding transboundary stocks’ availability by combining multiple fisheries-independent surveys and oceanographic conditions in spatiotemporal models. *ICES J. Mar. Sci.* **79**(4): 1063–1074. doi:10.1093/icesjms/fsac046.

Ormseth, O.A., and Norcross, B.L. 2009. Causes and consequences of life-history variation in North American stocks of Pacific cod. *ICES J. Mar. Sci.* **66**(2): 349–357. doi:10.1093/icesjms/fsn156.

Pedersen, M.W., Righton, D., Thygesen, U.H., Andersen, K.H., and Madsen, H. 2008. Geolocation of North Sea cod (*Gadus morhua*) using hidden Markov models and behavioural switching. *Can. J. Fish. Aquat. Sci.* **65**(11): 2367–2377. doi:10.1139/f08-144.

Perry, A.L., Low, P.J., Ellis, J.R., and Reynolds, J.D. 2005. Climate change and distribution shifts in marine fishes. *Science*, **308**(5730): 1912–1915. doi:10.1126/science.1111322. PMID: 15890845.

Pinheiro, J., and Bates, D. 2000. Mixed-effects models in S and S-PLUS. Springer-Verlag, New York.

Pinheiro, J., Bates, D., DebRoy, S., and Sarkar, D., Team, R.C. 2021. nlme: linear and nonlinear Mixed Effects Models. R package version 3.1-152.

Pinsky, M.L., Selden, R.L., and Kitchel, Z.J. 2020. Climate-driven shifts in marine species ranges: scaling from organisms to communities. *Annu. Rev. Mar. Sci.* **12**: 153–179. doi:10.1146/annurev-marine-010419-010916. PMID: 31505130.

R Core Team. 2023. R: A language and environment for statistical computing. R Foundation for Statistical Computing, Vienna.

Rand, K.M., Munro, P., Neidetcher, S.K., and Nichol, D.G. 2014. Observations of seasonal movement from a single tag release group of Pacific Cod in the eastern Bering Sea. *Mar. Coastal Fish.* **6**(1): 287–296. doi:10.1080/19425120.2014.976680.

Rohan, S.K., Barnett, L.A.K., and Charriere, N. 2022. Evaluating approaches to estimating mean temperatures and cold pool area from Alaska Fisheries Science Center bottom trawl surveys of the eastern Bering Sea. U.S. Dep. Commer., NOAA Tech. Memo. NMFS-AFSC-456, 42 p.

Rose, G.A., and Rowe, S. 2024. Northern cod re-establish historical migration patterns linked to capelin: insights from pop-up satellite archival tags. *Can. J. Fish. Aquat. Sci.* **81**(6): 646–669. doi:10.1139/cjfas-2023-0172.

Shimada, A., and Kimura, D. 1994. Seasonal movements of Pacific cod, *gadus macrocephalus*, in the eastern Bering Sea and adjacent waters based on tag-recapture data. *Fish. Bull.* **92**: 800–816.

Siddon, E. 2021. Ecosystem Status Report 2021: Eastern Bering Sea, stock assessment and Fishery Evaluation Report. North Pacific Fishery Management Council, 1007 West Third, Suite 400. Anchorage, Alaska. 99501.

Siddon, E. 2023. Ecosystem Status Report 2023: Eastern Bering Sea, stock assessment and Fishery Evaluation report. North Pacific Fishery Management Council, 1007 West Third, Suite 400, Anchorage, Alaska 99501.

Spies, I., Gruenthal, K.M., Drinan, D.P., Hollowed, A.B., Stevenson, D.E., Tarpey, C.M., and Hauser, L. 2020. Genetic evidence of a northward range expansion in the eastern Bering Sea stock of Pacific cod. *Evol. Appl.* **13**(2): 362–375. doi:[10.1111/eva.12874](https://doi.org/10.1111/eva.12874).

Stabeno, P.J., and Bell, S.W. 2019. Extreme conditions in the Bering Sea (2017–2018): Record-breaking low sea-ice extent. *Geophys. Res. Lett.* **46**: 8952–8959. doi:[10.1029/2019GL083816](https://doi.org/10.1029/2019GL083816)

Stafford, K.M., Farley, E.V., Ferguson, M., Kuletz, K.J., and Levine, R. 2022. Northward range expansion of subarctic upper trophic level animals into the Pacific Arctic region. *Oceanography*, **35**(3-4): 158–166. doi:[10.5670/oceanog.2022.101](https://doi.org/10.5670/oceanog.2022.101).

Stevenson, D.E., and Lauth, R.R. 2012. Latitudinal trends and temporal shifts in the catch composition of bottom trawls conducted on the eastern Bering Sea shelf. *Deep Sea Res. Part II Top. Stud. Oceanogr.* **65–70**: 251–259. doi:[10.1016/j.dsr2.2012.02.021](https://doi.org/10.1016/j.dsr2.2012.02.021).

Stevenson, D.E., and Lauth, R.R. 2019. Bottom trawl surveys in the northern Bering Sea indicate recent shifts in the distribution of marine species. *Polar Biol.* **42**: 407–421. doi:[10.1007/s00300-018-2431-1](https://doi.org/10.1007/s00300-018-2431-1).

Strøm, J.F., Bøhn, T., Skjæraasen, J.E., Gjelland, K.Ø., Karlsen, Ø., Johansen, T., et al. 2023. Movement diversity and partial sympatry of coastal and Northeast Arctic cod ecotypes at high latitudes. *J. Anim. Ecol.* **92**(10): 1966–1978. doi:[10.1111/1365-2656.13989](https://doi.org/10.1111/1365-2656.13989). PMID: [37485731](https://pubmed.ncbi.nlm.nih.gov/37485731/).

Sundby, S., and Nakken, O. 2008. Spatial shifts in spawning habitats of Arcto-Norwegian cod related to multidecadal climate oscillations and climate change. *ICES J. Mar. Sci.* **65**(6): 953–962. doi:[10.1093/icesjms/fsn085](https://doi.org/10.1093/icesjms/fsn085).

Szuwalski, C., Aydin, K., Fedewa, E., Garber-Yonts, B., and Litzow, M. 2023. The collapse of eastern Bering Sea snow crab. *Science*, **382**(6668): 306–310. doi:[10.1126/science.adf6035](https://doi.org/10.1126/science.adf6035).

Thompson, G.G., and Thorson, J.T. 2019. Assessment of the Pacific Cod stock in the Eastern Bering Sea. In Plan team for groundfish fisheries of the Bering Sea and Aleutian Islands (compiler), *Stock Assessment and Fishery Evaluation report for the groundfish resources of the Bering Sea and Aleutian Islands*. North Pacific Fishery Management Council.

Thygesen, U., Pedersen, M., and Madsen, H. 2009. Geolocating fish using hidden Markov models and data storage tags. In *Tagging and Tracking of Marine Animals with Electronic Devices*. Edited by J. Nielsen, H. Arrizabalaga, N. Fragoso, A. Hobday, M. Lutkavage and J. Sibert. Springer Netherlands. pp. 277–293.

U.S. National Ice Center. 2010. Multisensor Analyzed Sea Ice Extent—Northern Hemisphere (MASIE-NH), Version 1. National Snow and Ice Data Center. doi:[10.7265/N5GT5K3K](https://doi.org/10.7265/N5GT5K3K).

Wildlife Computers. 2012. WC-GPE2: Global Position Estimator Version 2. Wildlife Computers Inc., Redmond, Washington, USA.

Zuur, A.F., Ieno, E.N., Walker, N.J., Saveliev, A.A., and Smith, G.M. 2009. *Mixed effects models and extensions in ecology with R. Statistics for biology and health*. Springer, New York, NY.